Optimal absorption of acoustical waves by a boundary

Frédéric Magoulès, Thi Phuong Kieu Nguyen, Pascal Omnes, Anna Rozanova-Pierrat

Optimal absorption of acoustical waves by a boundary. Part I

Frédéric Magoulès[*], Thi Phuong Kieu Nguyen[*],
Pascal Omnes[†], Anna Rozanova-Pierrat[*]

January 19, 2018

[1] [2]

Abstract

In the aim to find the simplest and most efficient shape of a noise absorbing wall to dissipate the acoustical energy of a sound wave, we consider a frequency model described by the Helmholtz equation with a damping on the boundary. For a fixed porous material, considered as an acoustic absorbent, we find the damping boundary parameters from the corresponding time-depending problem, described by the damped wave equation (damping in volume). For the case of a regular boundary we provide the shape derivative of an objective function, chosen to describe the acoustical energy. Using the gradient method for the shape derivative, combined with the finite volume and level set methods, we find numerically the optimal shapes for a fixed frequency. We show the stability of the numerical algorithm and the non-uniqueness of the optimal shape, which can be explained by the non-uniqueness of the geometry providing the same spectral properties.

1 Introduction

The diffraction and absorption of waves by a system with both absorbing properties and irregular geometry is an open physical problem. This has to be solved to understand why anechoic chambers (electromagnetic or acoustic) do work better with irregular absorbing walls. Therefore there is a question about the existence of an optimal shape of an absorbent wall (for a fixed absorbing material), optimal in the sense that it is as dissipative as possible for a large range of frequencies, and at the same time that such a wall could effectively be constructed. In the framework of the propagation of acoustic waves, the acoustic absorbent material of the wall is considered as a porous medium. This article is

[1] Laboratoire de Mathématiques et Informatique pour la Complexité et les Systèmes, CentralSupélec, Université Paris-Saclay, 3 rue Joliot Curie, F-91192 Gif-sur-Yvette, France.

[2] CEA, DEN, DANS, DM2S, STMF, F-91191 Gif sur Yvette Cedex, France and Université Paris 13, Sorbonne Paris Cité, LAGA, CNRS (UMR 7539), 99 Avenue J.-B. Clément F-93430, Villetaneuse Cedex, France.

the first in a series of two. For a fixed frequency of the sound wave, we solve the shape optimization problem of minimizing the acoustical energy for a frequency model with a damping on the boundary. The question of optimal shapes for a finite or infinite range of frequencies is treated in Part II [18].

In the area of the optimization of acoustic performances of non absorbing walls, Duhamel [10, 11] studies sound propagation in a two dimensional vertical cut of a road wall and uses genetic algorithms to obtain optimal shapes (some of them are however not connected and thus could not be easily manufactured). The author also uses a branch and bound (combinatorial optimization) type linear programming in order to optimize the position sensors that allow an active noise control, firstly introduced by Lueg [15] in 1934. Abe et al. [1] consider a boundary elements based shape optimization of a non absorbing two-dimensional wall in the framework of a two-dimensional sound scattering problem for a fixed frequency (for the Helmholtz equation) using a topological derivative with the principle that a new shape or topology is obtained by nucleating small scattering bodies. Also for the Helmholtz equation for a fixed frequency, using the shape derivative of a functional representing the acoustical energy, Cao and Stanescu [8] consider a two-dimensional shape design problem for a non-absorbing part of the boundary to reduce the amount of noise radiated from aircraft turbofan engines. For the same problem, Farhadinia [13] developed a method based on measure theory, which does not require any information about gradients and the differentiability of the cost function.

On the other hand, for shape optimization problems there are a lot of theoretical results, reviewed in Refs. [3, 19], which rely on the topological derivatives of the cost functional to be minimized, with numerical application of the gradient method in both two and three dimensional cases (in the framework of solid mechanics). In this area, Achdou and Pironneau [2] considered the problem of optimization of a photocell, using a complex-valued Helmholtz system with periodic boundary conditions with the aim to maximize the solar energy in a dissipative region.

For acoustic waves in the two-dimensional case, optimization of the shape of an absorbing inclusion placed in a lossless acoustic medium was considered in Refs. [20, 21]. The considered model is the linear damped wave equation [9, 5], which we also consider in Part II [18]. Using the topology derivative approach, Münch et al. consider in [20, 21] the minimization of the acoustic energy of the solution of the damped wave equation at a given time $T > 0$ without any geometric restrictions and without the purpose of the design of an absorbent wall.

See also [4] for the shape optimization of shell structure acoustics.

In this article, we study the two-dimensional shape optimization problem for a Helmholtz equation with a damping on the boundary, modeled by a complex-valued Robin boundary condition (see system (3) and Fig. 2). The shape of the damping boundary is to be found, in the aim to minimize the total acoustical energy of the system. The noise source can be imposed as a source term in the equation and/or by a Dirichlet boundary condition (on the boundary opposite to the absorbing wall), which models a noise coming from a road. As for acoustical cavities, the domain of computation is limited on its top and bottom by boundaries with Neumann boundary conditions.

In Section 2, we introduce the frequency model and its time-dependent analogue with a dissipation on the boundary. We analyze its dissipative properties and give the well-

posedness results, due to [6, 14, 12, 3], useful for our shape optimization problem. We compare the model with dissipation by the boundary to the corresponding model with a dissipation in the volume, described by a damped wave equation in which the values of the coefficients for a given porous medium are given as functions of its macroscopic parameters (as porosity, tortuosity and resistivity to the passage of air), as initially proposed by [16]. In particular, in Theorem 4 proved in Appendix B, we propose a possible way to find the complex parameter in the Robin boundary condition of the former model that best approximates the latter. All numerical calculations, in particular in Section 6, are performed for a porous material named ISOREL, frequently used in building isolation (see A).

In Section 3, for the case of a regular boundary in the classical framework of shape optimization, for any fixed frequency we obtain the existence of an optimal shape.

For the case of a regular boundary we provide in Section 4 the shape derivative of an objective functional chosen to describe the acoustical energy. Using the gradient descent method for the shape derivative, combined with the finite volume and level set methods introduced in Section 5, we find numerically the optimal shapes for a fixed frequency. In Section 6, we show the stability of the numerical algorithm and the non-uniqueness of the optimal shape, which can be explained by the non-uniqueness of the geometry providing the same spectral properties.

2 The model: motivation and known properties

To describe the acoustic wave absorption by a porous medium, there are two possibilities. The first is to consider wave propagation in two media, typically the air and the wall, which corresponds to a damping in the volume. The most common mathematical model for it is the damped wave equation [5, 9]. The second possibility is to consider only one lossless medium, the air, and to model energy dissipation by a damping condition on the boundary. In both cases, we need to ensure the same order of energy damping corresponding to the physical characteristics of the chosen porous medium as its porosity ϕ, tortuosity α_h and resistivity to the passage of air σ [16].

Thanks to Ref. [16], we can define the coefficients in the damped wave equation (the case of the absorption in volume) as functions of the above mentioned characteristics. More precisely, for a regular bounded domain $\Omega \subset \mathbb{R}^2$ (for instance $\partial\Omega \in C^1$) composed of two disjoint parts $\Omega = \Omega_0 \cup \Omega_1$ of two homogeneous media, air in Ω_0 and a porous material in Ω_1, separated by an internal boundary Γ, we consider the following boundary value problem (for the pressure of the wave)

$$\begin{cases} \xi(x)\partial_t^2 u + a(x)\partial_t u - \nabla\cdot(\mu(x)\nabla u) = 0 \quad \text{in } \Omega, \\ \frac{\partial u}{\partial n}|_{\mathbb{R}_t\times\partial\Omega} \equiv 0, \quad [u]_\Gamma = [\mu\nabla u\cdot n]_\Gamma = 0, \\ u|_{t=0} = u_0 \mathbb{1}_{\Omega_0}, \quad \partial_t u|_{t=0} = u_1 \mathbb{1}_{\Omega_0}, \end{cases} \tag{1}$$

with $\xi(x) = \frac{1}{c_0^2}$, $a(x) = 0$, $\mu(x) = 1$ in the air (*i.e.* in Ω_0) and

$$\xi(x) = \frac{\phi\gamma_p}{c_0^2}, \quad a(x) = \sigma\frac{\phi^2\gamma_p}{c_0^2\rho_0\alpha_h}, \quad \mu(x) = \frac{\phi}{\alpha_h}$$

in the porous medium (*i.e.* in Ω_1). The external boundary $\partial\Omega$ is supposed to be perfectly rigid (Neumann boundary condition), and on the internal boundary Γ we have no-jump conditions on u and $\mu\nabla u \cdot n$, where n is the normal unit vector to Γ. Here, by c_0 and ρ_0 are respectively denoted the sound velocity in, and the density of the air, and by $\gamma_p = 7/5$ the ratio of specific heats. The damped character of the wave propagation, described by model (1), can be illustrated by the decreasing properties of the energy due to the damping term $a(x)u_t$ having its support in Ω_1:

$$\frac{1}{2}\frac{d}{dt}\left(\int_\Omega \left[\xi(\partial_t u)^2 + (\mu\nabla u)\cdot\nabla u\right]\mathrm{d}x\right) = -\int_{\Omega_1} a(\partial_t u)^2 \mathrm{d}x. \tag{2}$$

This model is numerically solved in Part II [18] Subsection 4.1.

But instead of the absorption in volume, especially for the sake of a simpler numerical treatment of the shape optimization, we consider the following frequency model of the damping by the boundary. Let Ω be a connected bounded domain of $\mathbb{R}^2$ with a Lipschitz boundary $\partial\Omega$. We suppose that the boundary $\partial\Omega$ is divided into three parts $\partial\Omega = \Gamma_D \cup \Gamma_N \cup \Gamma$ (see Fig. 2 for an example of Ω, chosen for the numerical calculations) and consider

$$\begin{cases} \triangle u + \omega^2 u = f(x), & x \in \Omega, \\ u = g(x) \quad \text{on } \Gamma_D, & \dfrac{\partial u}{\partial n} = 0 \quad \text{on } \Gamma_N, \quad \dfrac{\partial u}{\partial n} + \alpha(x)u = h(x) \quad \text{on } \Gamma, \end{cases} \tag{3}$$

where $\alpha(x)$ is a complex-valued regular function with a strictly positive real part ($\mathrm{Re}(\alpha) > 0$) and a strictly negative imaginary part ($\mathrm{Im}(\alpha) < 0$).

Remark 1 *This particular choice of the signs of the real and the imaginary parts of α are needed for the well-posedness properties and the energy decay of the corresponding time-dependent problem. In addition, as the frequency $\omega > 0$ is supposed to be fixed, α can contain a dependence on ω, i.e., $\alpha \equiv \alpha(x,\omega)$.*

Problem (3) is a frequency version of the following time-dependent wave propagation problem, considered in Ref. [6] for $g = 0$ on Γ_D:

$$\partial_t^2 u - \triangle u = -e^{-i\omega t} f(x), \tag{4}$$

$$u|_{t=0} = u_0, \quad \partial_t u|_{t=0} = u_1, \tag{5}$$

$$u|_{\Gamma_D} = g, \quad \left.\frac{\partial u}{\partial n}\right|_{\Gamma_N} = 0, \tag{6}$$

$$\frac{\partial u}{\partial n} - \frac{\mathrm{Im}(\alpha(x))}{\omega}\partial_t u + \mathrm{Re}(\alpha(x))u|_\Gamma = 0. \tag{7}$$

To show the energy decay, we follow Ref. [6] and introduce the Hilbert space $X_0(\Omega)$, defined as the Cartesian product of the set of functions $u \in H^1(\Omega)$, which vanish on Γ_D with the space $L_2(\Omega)$. The equivalent norm on $X_0(\Omega)$ is defined by

$$\|(u,v)\|^2_{X_0(\Omega)} = \int_\Omega \left(|\nabla_x u|^2 + |v|^2\right)\mathrm{d}x + \int_\Gamma \mathrm{Re}(\alpha(x))|u|^2 \mathrm{d}\sigma$$

with the corresponding inner product

$$\langle (u_1, u_2), (v_1, v_2) \rangle = \int_\Omega (\nabla_x u_1 \nabla_x v_1 + u_2 v_2) \, \mathrm{d}x + \int_\Gamma \mathrm{Re}(\alpha(x)) u_1 v_1 \mathrm{d}\sigma. \tag{8}$$

The advantage of this norm is that the energy balance of the homogeneous problem (4)–(7) has the form

$$\partial_t \left(\|(u, \partial_t u)\|^2_{X_0(\Omega)} \right) = \frac{2}{\omega} \int_\Gamma \mathrm{Im}(\alpha(x)) |\partial_t u|^2 \mathrm{d}s.$$

Therefore, for $\mathrm{Im}(\alpha) < 0$ on Γ, the energy decays in time.

For the case of a smooth boundary $\partial\Omega$ (at least Lipschitz), we have the well-posedness of both models. Thanks to Ref. [6], for all $f \in L^2(\Omega)$, $(u_0, u_1) \in X_0(\Omega)$ there exists a unique solution $(u, u_t) \in C(]0, \infty[, X_0(\Omega))$ of system (4)–(7) under the assumption that $\mathrm{Re}(\alpha(x)) > 0$ and $\mathrm{Im}(\alpha(x)) < 0$ are continuous functions.

For the frequency model (3) we introduce the space

$$V(\Omega) = \{ u \in H^1(\Omega) |\ u = 0 \text{ on } \Gamma_D \} \tag{9}$$

with the norm

$$\|u\|^2_{V(\Omega)} = \int_\Omega |\nabla u|^2 \mathrm{d}x + \int_\Gamma \mathrm{Re}(\alpha) |u|^2 \mathrm{d}m_d,$$

and we have the following well-posedness result:

Theorem 1 *(Gander et al. [14], Evans [12])Let $\Omega \subset \mathbb{R}^n$ be a bounded domain with a smooth (at least Lipschitz) boundary $\partial\Omega = \Gamma_D \cup \Gamma_N \cup \Gamma$. Let in addition $\mathrm{Re}(\alpha(x)) > 0$, $\mathrm{Im}(\alpha(x)) < 0$ be smooth functions (at least continuous) on Γ.*

Then for all $f \in L^2(\Omega)$, $g \in H^{1/2}(\Gamma_D)$ and $\omega > 0$ there exists a unique $u \in H^1(\Omega)$ solution of problem (3) with $h = 0$, continuously depending on the data: there exists a constant $C > 0$, not depending on f and g, such that

$$\|u\|_{H^1(\Omega)} \leq C \left(\|f\|_{L^2(\Omega)} + \|g\|_{H^{\frac{1}{2}}(\Gamma_D)} \right).$$

In addition, if, for $m \in \mathbb{N}^*$, $\partial\Omega \in C^{m+2}$, $f \in H^m(\Omega)$ and $g \in H^{m+\frac{3}{2}}(\Gamma_D)$, then the solution u belongs to $H^{m+2}(\Omega)$.

For the adjoint problem, i.e. with $g = 0$ and h, the trace of an element $\hat{h} \in V(\Omega)$, the Helmholtz problem (3) has a unique weak solution $u \in V(\Omega)$ for all $f \in L^2(\Omega)$ and $\hat{h} \in V(\Omega)$ in the following sense: for all $v \in V(\Omega)$

$$-\int_\Omega \nabla u \cdot \nabla \bar{v} \mathrm{d}x + \omega^2 \int_\Omega u \bar{v} \mathrm{d}x - \int_\Gamma \alpha u \bar{v} \mathrm{d}m_d = \int_\Omega f \bar{v} \mathrm{d}x - \int_\Gamma h \bar{v} \mathrm{d}m_d. \tag{10}$$

Moreover, the solution u continuously depends on the data: there exists a constant $C > 0$, independent of f, $\hat{h}$ and the values of α, such that

$$\|u\|_{V(\Omega)} \leq C \left(\|f\|_{L^2(\Omega)} + \|\hat{h}\|_{V(\Omega)} \right).$$

In addition, if, for $m \in \mathbb{N}^*$, $\partial\Omega \in C^{m+2}$, $f \in H^m(\Omega)$ and $\hat{h} \in H^{m+1}(\Omega) \cap V(\Omega)$, then the weak solution u belongs to $H^{m+2}(\Omega) \cap V(\Omega)$.

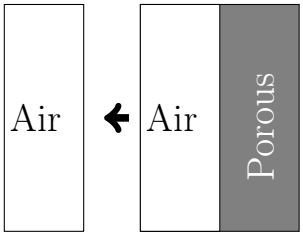

Figure 1: One medium for the absorption on the boundary (left) and two media for the absorption in the volume (right).

In order to relate the model with a damping on the boundary and the model with a damping in the volume (see Fig. 1), we propose in Theorem 4 (see the supplementary materials for the proof) a way to identify the parameter α in the Robin boundary condition that provides the best approximation (in some error minimizing sense) of the latter model by the former, in the case of a flat boundary Γ.

3 Shape design problem

We consider the two dimensional shape design problem, which consists in optimizing the shape of Γ with the Robin dissipative condition in order to minimize the acoustic energy of system (3). The boundaries with the Neumann and Dirichlet conditions Γ_D and Γ_N are supposed to be fixed. We denote by Ω_0 and Γ_0 the domain and the boundary respectively of the initial shape before optimization. The optimization step modifies the initial shape of Γ_0 to $\Gamma = (Id + \theta)\Gamma_0$, according to the map $x \in \Gamma_0 \mapsto (x + \theta(x)) \in \Gamma$ and following the vector field $\theta \in W^{1,\infty}(\mathbb{R}^2, \mathbb{R}^2)$. Here Id is the identity map $x \in \mathbb{R}^2 \mapsto x \in \mathbb{R}^2$, $W^{1,\infty}(\mathbb{R}^2, \mathbb{R}^2)$ is the space of Lipschitz functions ϕ from $\mathbb{R}^2$ to $\mathbb{R}^2$, such that ϕ and $\nabla\phi$ are uniformly bounded in $\mathbb{R}^2$. Using the notations $|\cdot|_{\mathbb{R}^2}$ for the Euclidean norm in $\mathbb{R}^2$ and $|\cdot|_{\mathbb{R}^{2\times 2}}$ for the matrices Euclidean norm on $\mathbb{R}^2$, we define the norm on $W^{1,\infty}(\mathbb{R}^2, \mathbb{R}^2)$ by

$$\|\phi\|_{W^{1,\infty}(\mathbb{R}^2,\mathbb{R}^2)} = \sup_{x\in\mathbb{R}^2} \left(|\phi(x)|_{\mathbb{R}^2} + |\nabla\phi(x)|_{\mathbb{R}^{2\times 2}}\right).$$

Hence $\left(W^{1,\infty}(\mathbb{R}^2, \mathbb{R}^2), \|\cdot\|_{W^{1,\infty}(\mathbb{R}^2,\mathbb{R}^2)}\right)$ is a Banach space. Following Ref. [3], p. 127, we also define for a fixed open set D with a Lipschitz boundary the space

$$\mathcal{C}_D(\Omega_0) = \{\Omega \subset D \subset \mathbb{R}^2 |\ \exists\theta \in W^{1,\infty}(\mathbb{R}^2, \mathbb{R}^2),\ \|\theta\|_{W^{1,\infty}(\mathbb{R}^2,\mathbb{R}^2)} < 1 \text{ such that } \Omega = (Id + \theta)\Omega_0\}.$$

Actually, as only a part of the boundary (precisely Γ) changes its shape, we can also impose that the changing part always lies inside of the closure of a fixed open set G with a Lipschitz boundary: $\Gamma \subset \overline{G}$ (see the example of Fig. 2). The set G forbids Γ to be too close to Γ_D, what makes the idea of an acoustical wall more realistic. Thus, we define the space

$$\mathcal{C}(\Omega_0) = \{\Omega \in \mathcal{C}_D(\Omega_0) |\ \Gamma \subset \overline{G}\}. \tag{11}$$

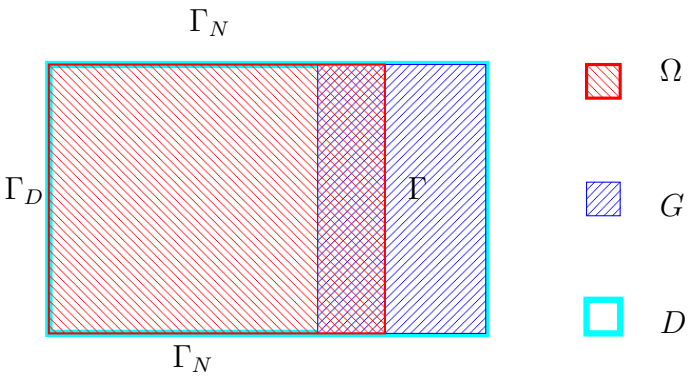

Figure 2: Example of a domain Ω in $\mathbb{R}^2$ with three types of boundaries: Γ_D and Γ_N are fixed and Γ can be changed in the restricted area $\overline{G}$. Here $\Omega \cup G = D$ and obviously $\Omega \subset D$.

To introduce the class of admissible domains, on which we minimize the acoustical energy of system (3), we define [3, 22] the quasi-distance $d(\Omega, \Omega_0)$ on $\mathcal{C}(\Omega_0)$

$$d(\Omega, \Omega_0) = \inf_{T \in \mathcal{T} | T(\Omega_0) = \Omega} (\|T - Id\|_{W^{1,\infty}(\mathbb{R}^2,\mathbb{R}^2)} + \|T^{-1} - Id\|_{W^{1,\infty}(\mathbb{R}^2,\mathbb{R}^2)})$$

with the following space of diffeomorphisms on $\mathbb{R}^2$:

$$\mathcal{T} = \{T |\ (T - Id) \in W^{1,\infty}(\mathbb{R}^2, \mathbb{R}^2),\ T^{-1} - Id \in W^{1,\infty}(\mathbb{R}^2, \mathbb{R}^2)\}.$$

Typically $T = Id + \theta$ with $\|\theta\|_{W^{1,\infty}(\mathbb{R}^2,\mathbb{R}^2)} < 1$. If $d_H(\Omega_0, \Omega)$ is the Hausdorff distance between Ω_0 and Ω, we know [22] that $d_H(\Omega_0, \Omega) \leq d(\Omega_0, \Omega)$. Hence, in what follows, our purpose is to minimize the acoustic energy in Ω over all admissible shapes Γ, keeping constant the volume of the initial domain Ω_0, *i.e.* we want to minimize

$$J(\Omega, u) = A \int_\Omega |u|^2 \mathrm{d}x + B \int_\Omega |\nabla u|^2 \mathrm{d}x + C \int_\Gamma |u|^2 d\sigma \tag{12}$$

for the domains $\Omega \in U_{ad}(\Omega_0)$ from the admissible class of domains

$$U_{ad}(\Omega_0) = \{\Omega \in \mathcal{C}(\Omega_0) | d(\Omega, \Omega_0) \leq \frac{1}{8},\ \Gamma_D \cup \Gamma_N \subset \partial\Omega,\ \int_\Omega \mathrm{d}x = \mathrm{Vol}(\Omega_0)\} \tag{13}$$

with $\mathrm{Vol}(\Omega_0) = |\Omega_0| = \int_{\Omega_0} \mathrm{d}x$, $A \geq 0$, $B \geq 0$, $C \geq 0$ positive constants for all fixed $\omega > 0$. In what follows we also suppose that A, B and C are regular functions of ω:

Example 1 *Let* $\mathrm{Re}(\alpha(\omega))$ *be independent on* x. *If* J *is the acoustic energy of the Helmholtz problem (3), we typically have* $A = 1$, $B = C = 0$ *or equivalently, thanks to the variational form,* $A = 0$, $B = \frac{1}{\omega^2}$, $C = \frac{\mathrm{Re}(\alpha(\omega))}{\omega^2}$.

In the definition of U_{ad} we take $d(\Omega, \Omega_0) \leq \frac{1}{8}$, according to Lemma 2.4 in Ref. [22] in the case $n = 2$ and $k = 1$. The restriction that all admissible domains $\Omega \in U_{ad}$ have the

fixed parts Γ_D and Γ_N in their boundaries is taken into account in the parametrization of $\Omega = (Id + \theta)\Omega_0$ by the vector field θ. It is sufficient to impose $\theta = 0$ on $\Gamma_D \cup \Gamma_N$, meaning that only the part Γ of the boundary may vary. In order to keep the volume constraint, instead of Eq. (12) we can also consider the objective function

$$J_1(\Omega, u) = A \int_\Omega |u|^2 \mathrm{d}x + B \int_\Omega |\nabla u|^2 \mathrm{d}x + C \int_\Gamma |u|^2 d\sigma + \mu(\mathrm{Vol}(\Omega) - \mathrm{Vol}(\Omega_0))^2, \qquad (14)$$

where μ is some (large) positive constant penalizing the volume variation.

Following the approach of F. Murat and J. Simon [22], also explained in Ref. [17], we have, using the continuity of u and J as functions of Ω [17], the existence of an optimal shape:

Theorem 2 *Let $\Omega_0 \subset D$ be a domain with a Lipschitz boundary $\partial\Omega_0$ such that $\Gamma_D \cup \Gamma_N \subset \partial\Omega_0$, U_{ad} be defined by (13) and $\omega > 0$ be fixed. For the objective function $J(\Omega)$, defined in (12), the shape optimization problem $\inf_{\Omega \in U_{ad}(\Omega_0)} J(\Omega)$ has at least one minimum point (there exists at least one optimal shape Γ).*

See also Ref. [7] for a free discontinuity approach to a class of shape optimization problems involving Robin condition on a free boundary.

4 Shape derivative

Following the ideas in Ref. [3], we provide two types of derivation of J_1 with respect to the shape of Ω: the first method is a formal derivation of the Lagrangian, associated with the optimization problem, which allows in the simplest way to obtain formula (16) below, but does not allow to prove it rigorously. To have a rigorous proof, as it is explained in Ref. [3], we need to use a direct derivative approach, involving the Eulerian derivative with respect to the domain, which is much more complicated. Both methods give the same formula (16). Let us start by introducing the definition of the shape derivative of a function (see Ref. [3]). Without lost of generality, we always consider the two dimensional case $(n = 2)$.

Definition 1 (Shape derivative) *The shape derivative of a function $K(\Omega) : \mathcal{C}(\Omega_0) \to \mathbb{R}$ at Ω_0 is defined as the Fréchet derivative in $W^{1,\infty}(\mathbb{R}^2, \mathbb{R}^2)$ at 0 of the function $\theta \mapsto K\left(Id + \theta\right)(\Omega_0)$, i.e.,*

$$K\left(Id + \theta\right)(\Omega_0) = K(\Omega_0) + K'(\Omega_0)(\theta) + o(\theta) \quad \textit{with} \quad \lim_{\theta \to 0} \frac{\|o(\theta)\|_{L^\infty(\mathbb{R}^2)}}{\|\theta\|_{W^{1,\infty}(\mathbb{R}^2,\mathbb{R}^2)}} = 0,$$

where $K'(\Omega_0)$ is a continuous linear form on $W^{1,\infty}(\mathbb{R}^2, \mathbb{R}^2)$.

As in Ref. [3], let us introduce the Eulerian derivative (or shape derivative), denoted by U.

Definition 2 (Eulerian derivative) *Assume that x belongs both to the initial domain Ω_0 and to the deformed domain $\Omega = (Id + \theta)(\Omega_0)$. A continuous linear form of $\theta \in$*

$W^{1,\infty}(\mathbb{R}^2,\mathbb{R}^2)$, *denoted by* $U(\theta,x)$, *is called the Eulerian derivative, if it is defined by the expression:*

$$u\left((Id+\theta)(\Omega_0),x\right)=u(\Omega_0,x)+U(\theta,x)+o(\theta),\ \ with\ \lim_{\theta\to 0}\frac{\|o(\theta)\|_{L^\infty(\mathbb{R}^2)}}{\|\theta\|_{W^{1,\infty}(\mathbb{R}^2,\mathbb{R}^2)}}=0, \tag{15}$$

i.e., U *is the directional derivative of* u *in the direction* θ.

We recall two important results from Ref. [3], which we use to compute the shape derivative of the objective functions J and J_1.

Lemma 1 (G. Allaire [3] Remark 6.29 p. 138) *Let* Ω_0 *be an open bounded smooth domain in* $\mathbb{R}^2$. *Let* $u(\Omega)$ *be a function from* $C(\Omega_0)$ *to* $L^1(\mathbb{R}^2)$. *Then the function* K_1 *from* $C(\Omega_0)$ *to* $\mathbb{R}$, *defined by*

$$K_1(\Omega)=\int_\Omega u(\Omega)\mathrm{d}x,$$

is differentiable at Ω_0 *and for all* $\theta\in W^{1,\infty}(\mathbb{R}^2,\mathbb{R}^2)$, *we have*

$$K_1'(\Omega_0)(\theta)=\int_{\Omega_0}\left(U(\theta)+\mathrm{div}(u(\Omega_0)\theta)\right)\mathrm{d}x.$$

Similarly, if $\hat{u}(\theta)$ *is derivable at* 0 *as function from* $C^1(\mathbb{R}^2,\mathbb{R}^2)$ *to* $L^1(\partial\Omega_0)$, *then*

$$K_2(\Omega)=\int_{\partial\Omega}u(\Omega)\mathrm{d}s$$

is differentiable at Ω_0 *and, for all* $\theta\in C^1(\mathbb{R}^2,\mathbb{R}^2)$, *we have*

$$K_2'(\Omega_0)(\theta)=\int_{\partial\Omega_0}\left(U(\theta)+\theta\cdot n\left(\frac{\partial u(\Omega_0)}{\partial n}+Hu(\Omega_0)\right)\right)\mathrm{d}s.$$

We prove the following theorem:

Theorem 3 *Let* Ω_0 *be a bounded domain in* $\mathbb{R}^2$ *with a connected boundary* $\partial\Omega_0\in C^3$, *divided in three disjoint parts* $\partial\Omega_0=\Gamma_0\sqcup\Gamma_D\sqcup\Gamma_N$. *Let* $\Omega\in\mathcal{C}(\Omega_0)$, *defined in (11), and such that* $\partial\Omega=\Gamma\sqcup\Gamma_D\sqcup\Gamma_N$ *with* $\Gamma=(Id+\theta)\Gamma_0$ *(*$\theta\in W^{2,\infty}(\mathbb{R}^2,\mathbb{R}^2)$ *and* $\|\theta\|<1$*). Let* $u(\Omega_0)\in H^3(\Omega_0)$ *be the solution of problem (3) in* Ω_0 *with* $g\in H^{\frac{5}{2}}(\Gamma_D)$ *and* $f\in H^1(\mathbb{R}^2)$ *(see Theorem 1). Then the shape derivative of the objective function* J_1, *defined in Eq. (14), is given by*

$$J_1'(\Omega_0)(\theta)=\int_{\Gamma_0}(\theta\cdot n)(-\mathcal{V})\mathrm{d}s, \tag{16}$$

where by the velocity $-\mathcal{V}$ *is denoted*

$$\begin{aligned}-\mathcal{V}=&\left(A|u|^2+B|\nabla u|^2+2B|\alpha|^2|u|^2-4C\mathrm{Re}(\alpha)|u|^2+CH|u|^2\right)\\&+\mathrm{Re}\left(-\nabla u\cdot\nabla w+\omega^2uw-fw-\alpha Huw+2\alpha^2uw\right)\\&+2\mu\left(\mathrm{Vol}(\Omega)-\mathrm{Vol}(\Omega_0)\right)\end{aligned} \tag{17}$$

with n *the exterior normal vector on* Γ_0, H *the curvature of the boundary* Γ_0, *and* $w\in V(\Omega_0)$ *(*$V(\Omega_0)$ *is defined in Eq. (9)), the unique solution of the adjoint problem (see Eq. (22)) corresponding to* u.

4.1 Formal proof of Theorem 3 using the Lagrangian

Since the data of the problem and the solution u are complex functions (except ω which is a positive constant), let us separate the imaginary and real parts, adopting the following notation: $u = u_R + iu_I$. Thus, the boundary value problem for the Helmholtz equation (3) takes the following form:

$$\begin{aligned}
&\triangle u_R + \omega^2 u_R = f_R(x) \quad x \in \Omega, && (18)\\
&u_R = g_R(x) \quad \text{on } \Gamma_D, \quad \frac{\partial u_R}{\partial n} = 0 \quad \text{on } \Gamma_N, \quad \frac{\partial u_R}{\partial n} + \alpha_R u_R - \alpha_I u_I = 0 \quad \text{on } \Gamma,\\
&\triangle u_I + \omega^2 u_I = f_I(x) \quad x \in \Omega, && (19)\\
&u_I = g_I(x) \quad \text{on } \Gamma_D, \quad \frac{\partial u_I}{\partial n} = 0 \quad \text{on } \Gamma_N, \quad \frac{\partial u_I}{\partial n} + \alpha_I u_R + \alpha_R u_I = 0 \quad \text{on } \Gamma.
\end{aligned}$$

The objective function is considered as a function of the real and the complex parts of u:

$$\begin{aligned}
J(\Omega, u_R, u_I) =& A \int_\Omega \left(|u_R|^2 + |u_I|^2\right) \mathrm{d}x + B \int_\Omega \left(|\nabla u_R|^2 + |\nabla u_I|^2\right) \mathrm{d}x\\
&+ C \int_\Gamma \left(|u_R|^2 + |u_I|^2\right) \mathrm{d}s.
\end{aligned}$$

We write down the variational formulations for (18) and (19) and substract them to obtain for all $(w_R, w_I) \in V(\Omega) \times V(\Omega)$

$$\begin{aligned}
&- \int_\Gamma \left(\left(\alpha_R u_R - \alpha_I u_I\right) w_R - \left(\alpha_I u_R + \alpha_R u_I\right) w_I\right) \mathrm{d}s\\
&+ \int_\Omega \left(\nabla u_I \nabla w_I - \nabla u_R \nabla w_R + \omega^2 \left(u_R w_R - u_I w_I\right) + f_I w_I - f_R w_R\right) \mathrm{d}x = 0. \qquad (20)
\end{aligned}$$

We define (see [3] p. 152) the Lagrangian of the optimization problem as the sum of the functional J and the variational formulation (20)

$$\begin{aligned}
&L(\Omega, u_R, u_I, w_R, w_I) = A \int_\Omega (|u_R|^2 + |u_I|^2) \mathrm{d}x\\
&+ B \int_\Omega (|\nabla u_R|^2 + |\nabla u_I|^2) \mathrm{d}x + C \int_\Gamma \left(|u_R|^2 + |u_I|^2\right) \mathrm{d}s\\
&+ \int_\Omega \left(\nabla u_I \nabla w_I - \nabla u_R \nabla w_R + \omega^2 \left(u_R w_R - u_I w_I\right) + f_I w_I - f_R w_R\right) \mathrm{d}x\\
&- \int_\Gamma \left(\left(\alpha_R u_R - \alpha_I u_I\right) w_R - \left(\alpha_I u_R + \alpha_R u_I\right) w_I\right) \mathrm{d}s, \qquad (21)
\end{aligned}$$

where u_R, u_I, w_R and w_I are in $V(\Omega)$. The conjugate problem can be found from the system

$$\left\langle \frac{\partial L}{\partial u_R}, \psi_R \right\rangle = 0, \quad \left\langle \frac{\partial L}{\partial u_I}, \psi_I \right\rangle = 0,$$

with

$$\left\langle \frac{\partial L}{\partial u_R}, \psi_R \right\rangle = \int_\Omega (2Au_R\psi_R + 2B\nabla u_R \nabla\psi_R - \nabla w_R \nabla\psi_R + \omega^2 w_R\psi_R)\mathrm{d}x \\ - \int_\Gamma (\alpha_R w_R - \alpha_I w_I - 2Cu_R)\,\psi_R \mathrm{d}s$$

and

$$\left\langle \frac{\partial L}{\partial u_I}, \psi_I \right\rangle = \int_\Omega (2Au_I\psi_I + 2B\nabla u_I \nabla\psi_I + \nabla w_I \nabla\psi_I - \omega^2 w_I\psi_I)\mathrm{d}x \\ + \int_\Gamma (\alpha_I w_R + \alpha_R w_I + 2Cu_I)\,\psi_I \mathrm{d}s.$$

This is the variational formulation of the following adjoint problem:

$$\begin{cases} \triangle w_R + \omega^2 w_R = -2(Au_R(\Omega_0) - B\triangle u_R(\Omega_0)) \quad x \in \Omega_0, \\ w_R = 0 \quad \text{on } \Gamma_D, \quad \dfrac{\partial w_R}{\partial n} = 0 \quad \text{on } \Gamma_N, \\ \dfrac{\partial w_R}{\partial n} + \alpha_R w_R - \alpha_I w_I = -2B[\alpha_R u_R(\Omega_0) - \alpha_I u_I(\Omega_0)] + 2Cu_R(\Omega_0) \quad \text{on } \Gamma_0, \\ \triangle w_I + \omega^2 w_I = 2(Au_I(\Omega_0) - B\triangle u_I(\Omega_0)) \quad x \in \Omega_0, \\ w_I = 0 \quad \text{on } \Gamma_D, \quad \dfrac{\partial w_I}{\partial n} = 0 \quad \text{on } \Gamma_N, \\ \dfrac{\partial w_I}{\partial n} + \alpha_I w_R + \alpha_R w_I = 2B(\alpha_R u_I(\Omega_0) + \alpha_I u_R(\Omega_0)) - 2Cu_I(\Omega_0) \quad \text{on } \Gamma_0. \end{cases} \tag{22}$$

We notice that the adjoint problem (22) can be more compactly rewritten for the complex-valued functions $w \in V(\Omega_0)$ ($w = w_R + iw_I$), $u(\Omega_0)$ and α:

$$\begin{cases} \triangle w + \omega^2 w = -2\left(A\bar{u}(\Omega_0) - B\triangle\bar{u}(\Omega_0)\right) \; x \in \Omega_0, \\ w = 0 \quad \text{on } \Gamma_D, \quad \dfrac{\partial w}{\partial n} = 0 \quad \text{on } \Gamma_N, \\ \dfrac{\partial w}{\partial n} + \alpha w = -2B\bar{\alpha}\bar{u}(\Omega_0) + 2C\bar{u}(\Omega_0) \quad \text{on } \Gamma_0. \end{cases} \tag{23}$$

Hence, thanks to [3] Proposition 6.22 on p. 134 and Proposition 6.24 on p. 135, $J'(\Omega_0)(\theta)$ is given by the derivative of (21) over Ω:

$$\begin{aligned} J'(\Omega_0)(\theta) &= \frac{\partial L}{\partial \Omega}(\Omega_0, u_R, u_I, w_R, w_I)(\theta) \\ &= \int_{\Gamma_0} \theta\cdot n \left(A|u|^2 + B|\nabla u|^2 - 2C\mathrm{Re}(\alpha)|u|^2 + CH|u|^2\right)\mathrm{d}s \\ &+ \int_{\Gamma_0} \theta\cdot n \mathrm{Re}\left(-\nabla u\cdot\nabla w + \omega^2 uw - fw - \alpha Huw - \alpha\frac{\partial(uw)}{\partial n}\right)\mathrm{d}s, \end{aligned} \tag{24}$$

where n is the outward normal on Γ_0 and H is the curvature of Γ_0. Using the boundary conditions and adding the volume constraint, we directly obtain (16).

4.2 Rigorous proof of Theorem 3

Since Γ_D does not move in our assumption, and thus, the value g does not have any influence on the shape derivative $J'(\Omega_0)$, in what follows, in the aim to simplify the notations, we take $g \equiv 0$ on Γ_D.

Let us follow the proof of Theorem 6.38 pp. 145–146 of G. Allaire [3] (see also on p. 144 the proof of Corollary 6.36).

Thanks to Lemma 1, we find the shape derivative of J as

$$\begin{aligned}
J'(\Omega_0)(\theta) &= \int_{\Omega_0} \operatorname{div}\left(\theta\left(A|u(\Omega_0)|^2 + B|\nabla u(\Omega_0)|^2\right)\right)\mathrm{d}x \\
&\quad + C\int_{\Gamma_0} \theta\cdot n\left(\frac{\partial|u(\Omega_0)|^2}{\partial n} + H|u(\Omega_0)|^2\right)\mathrm{d}s + 2C\int_{\Gamma_0}\mathrm{Re}(\bar{u}(\Omega_0)U)\mathrm{d}s \\
&\quad + \int_{\Omega_0}\left(2A\mathrm{Re}(\bar{u}(\Omega_0)U) + 2B\mathrm{Re}(\nabla\bar{u}(\Omega_0)\cdot\nabla U)\right)\mathrm{d}x \\
&= \int_{\Gamma_0}\theta\cdot n\left(A|u(\Omega_0)|^2 + B|\nabla u(\Omega_0)|^2 + C\frac{\partial|u(\Omega_0)|^2}{\partial n} + CH|u(\Omega_0)|^2\right)\mathrm{d}s \\
&\quad + \int_{\Omega_0}\mathrm{Re}\left(2A\bar{u}(\Omega_0)U + 2B\nabla\bar{u}(\Omega_0)\cdot\nabla U\right)\mathrm{d}x + 2C\int_{\Gamma_0}\mathrm{Re}(\bar{u}(\Omega_0)U)\mathrm{d}s, \quad (25)
\end{aligned}$$

where U is the Eulerian derivative. We need now to precise the real part of the variational formulation for the adjoint problem (see system (23)) taking $\overline{U}$ as the test function:

$$\begin{aligned}
&\mathrm{Re}\left(\int_{\Omega_0}\nabla w\nabla U\mathrm{d}x - \omega^2\int_{\Omega_0} wU\mathrm{d}x + \int_{\Gamma_0}\alpha wU\mathrm{d}s\right) \\
&\qquad = \int_{\Omega_0}\mathrm{Re}\left(2A\bar{u}(\Omega_0)U + 2B\nabla\bar{u}(\Omega_0)\nabla U\right)\mathrm{d}x + 2C\int_{\Gamma_0}\mathrm{Re}(\bar{u}(\Omega_0)U)\mathrm{d}s. \quad (26)
\end{aligned}$$

We notice that in the right-hand side (as the source terms) of (26) we have all integrals from (25) involving U.

Thanks to the regularity of the boundary $\partial\Omega$, the elements of $H^1(\Omega)$ can be considered as the restrictions of the corresponding elements of $H^1(\mathbb{R}^2)$. Thus, we can reformulate the variational form (10) by "find $u(\Omega) \in V(\mathbb{R}^2)$, such that for all $v \in V(\mathbb{R}^2)$ it holds

$$-\int_{\Omega}\nabla u\cdot\nabla\bar{v}\mathrm{d}x + \omega^2\int_{\Omega} u\bar{v}\mathrm{d}x - \int_{\Gamma}\alpha u\bar{v}\mathrm{d}\sigma = \int_{\Omega} f\bar{v}\mathrm{d}x."$$

We derive the last equality in Ω_0, using Lemma 1 and the facts, that $\theta = 0$ on Γ_D and Γ_N. Hence, we find that $u'(\Omega_0)(\theta) = U$, the Eulerian derivative of u, verifies for all $v \in V(\Omega_0)$

$$\begin{aligned}
&\int_{\Omega_0}(-\nabla U\cdot\nabla\overline{v} + \omega^2 U\overline{v})\mathrm{d}x - \int_{\Gamma_0}\alpha U\overline{v}\mathrm{d}s \\
&= \int_{\Gamma_0}\theta\cdot n\left(\nabla u\cdot\nabla\overline{v} - \omega^2 u\overline{v} + f\overline{v} + \alpha Hu\overline{v} + \alpha\frac{\partial(u\overline{v})}{\partial n}\right)\mathrm{d}s. \quad (27)
\end{aligned}$$

In particular (27) holds for $v = \overline{w}$, with w the weak solution of the adjoint problem (23).

Hence, from (27) with $v = \overline{w}$ and from (26) we find

$$\int_{\Omega_0} \mathrm{Re}\left(2A\bar{u}(\Omega_0)U + 2B\nabla\bar{u}(\Omega_0)\nabla U\right)\mathrm{d}x + \int_{\Gamma_0} 2C\mathrm{Re}(\bar{u}(\Omega_0)U)\mathrm{d}s$$
$$= \int_{\Gamma_0} \theta\cdot n\mathrm{Re}\left(-\nabla u(\Omega_0)\cdot\nabla w + \omega^2 u(\Omega_0)w - fw - \alpha H u(\Omega_0)w - \alpha\frac{\partial(u(\Omega_0)w)}{\partial n}\right)\mathrm{d}s.$$

Finally, by inserting the above formula into (25) and using the following equality inferred from the Robin boundary conditions for u and w on Γ_0:

$$\alpha\nabla(uw)\cdot n = \alpha\left(w\nabla u\cdot n + u\nabla w\cdot n\right) = -2\alpha^2 uw - 2B|\alpha|^2|u|^2 + 2C\alpha|u|^2,$$

we obtain that

$$J'(\Omega_0)(\theta) = \int_{\Gamma_0} \theta\cdot n\left(A|u(\Omega_0)|^2 + B|\nabla u(\Omega_0)|^2 + 2B|\alpha|^2|u(\Omega_0)|^2\right.$$
$$\left.-4C\mathrm{Re}(\alpha)|u(\Omega_0)|^2 + CH|u(\Omega_0)|^2\right)\mathrm{d}s$$
$$+\int_{\Gamma_0} \theta\cdot n\mathrm{Re}\left(-\nabla u(\Omega_0)\cdot\nabla w + \omega^2 u(\Omega_0)w - fw - \alpha H u(\Omega_0)w + 2\alpha^2 u(\Omega_0)w\right)\mathrm{d}s.$$

Now, if we add to the objective function the volume constraint with the Lagrange coefficient μ (see (14))

$$J_1(\Omega, u) = J(\Omega, u) + \mu\left(\mathrm{Vol}(\Omega) - \mathrm{Vol}(\Omega_0)\right)^2,$$

the shape derivative of the objective function J_1 is given by

$$J_1'(\Omega_0)(\theta) = J'(\Omega_0)(\theta) + 2\mu\int_{\Gamma_0}\theta\cdot n\left(\mathrm{Vol}(\Omega) - \mathrm{Vol}(\Omega_0)\right)\mathrm{d}s,$$

which concludes the proof of Theorem 3.

5 Shape optimization algorithm

We want to solve numerically, using the gradient descent method, the following minimization problem: for $\omega > 0$ and Ω_0 given, find $\Omega^{\mathrm{opt}} \in U_{ad}(\lambda, \Omega_0)$, such that

$$J_1(\Omega^{\mathrm{opt}}) = \min_{\Omega\in U_{ad}(\lambda,\Omega_0)} J_1(\Omega).$$

We notice that if the velocity $\mathcal{V}$, defined in Eq. (17, follows the outward normal direction, or equivalently, if $\theta\cdot n = \mathcal{V}$, then Eq. (16 implies that

$$J_1'(\Omega_0)(\theta) = -\int_{\Gamma_0}\mathcal{V}^2\mathrm{d}s < 0,$$

which ensures the decreasing behavior of the objective function. To calculate it, we need to know u, the solution of the Helmholtz equation in Ω_0, but also w, the solution of the adjoint problem and the curvature H. Inspired by Refs. [3, 24, 25], we construct a shape optimization algorithm composed of the following steps:

(i) Solving the Helmholtz (3) and its adjoint (23) problems by a cell-centered finite difference scheme on a square Cartesian mesh covering Ω.

(ii) Calculating the velocity $\mathcal{V}$ of the Robin boundary Γ, based on formula (17), and then extending this velocity in the direction of the normal vector on the whole domain D, or at least around the Robin boundary.

(iii) Solving the level set equation to obtain a new shape.

If $J_1'(\Omega)(\theta) \geq 0$, then Ω is an optimal domain, and the algorithm stops. In order to describe the shape of the domain, we use a concept of level sets. More precisely, the level set function ψ of the domain $\Omega \subset D$ is defined by

$$\begin{cases} \psi(x) = 0 & \text{iff} \quad x \in (\partial\Omega \cap D), \\ \psi(x) < 0 & \text{iff} \quad x \in \Omega, \\ \psi(x) > 0 & \text{iff} \quad x \in (D \setminus \Omega). \end{cases}$$

The level set method, initially devised by S. Osher and J-A. Sethian in Ref. [24], allows, not only to define implicitly the domain, but also to follow easily the propagation of the boundary during the evolution process. Let us take into account a particle $x(t)$ on the boundary, which propagates in time, hence it has the zero-level set all time, *i.e.*, $\psi(x(t), t) = 0$. By the chain rule, it yields that

$$\psi_t + x'(t) \cdot \nabla\psi\,(x(t), t) = 0. \tag{28}$$

If $\mathcal{V}$ is the velocity in the outward normal direction of the boundary, *i.e.* $x'(t) \cdot n = \mathcal{V}$, with $n = \frac{\nabla\psi}{|\nabla\psi|}$, then from Eq. (28, we obtain a so-called level set equation

$$\psi_t + \mathcal{V}|\nabla\psi| = 0, \tag{29}$$

associated with the initial condition $\psi|_{t=0} = \psi_0(x)$, defined by the signed distance function

$$\psi_0(x) = \pm \mathrm{dist}[x, \Gamma], \quad x \in D. \tag{30}$$

In the last formula, Γ is the Robin boundary, and the sign plus (or minus) corresponds to outside (or inside) of the domain Ω. This equation is of Hamilton-Jacobi type, and in what follows we call it the Hamilton-Jacobi equation. Let us notice, that we need to calculate the solution of he Hamilton-Jacobi equation (29) not only in Ω, but in D, and thus, we need to know $\mathcal{V}$ for all $x \in D$. Hence, knowing initially $\mathcal{V}$ only in Ω by formula (17), we need to extend it to all D. More precisely, to calculate numerically $-\mathcal{V}$ on Ω (see Eq. (17)), we first find numerically the solutions u of the Helmholtz problem (3) and w of the adjoint problem (23) and then evaluate ∇u and ∇w. The curvature H is calculated, on the basis of the level set function ψ, by the following equality

$$H = \nabla \cdot \frac{\nabla\psi}{|\nabla\psi|} = \frac{\psi_{yy}\psi_x^2 - 2\psi_x\psi_y\psi_{xy} + \psi_{xx}\psi_y^2}{\left(\psi_x^2 + \psi_y^2\right)^{3/2}}.$$

Once we know $\mathcal{V}$ in Ω, we extend it outside of the domain [23, 25], solving until the stationary state the equation

$$\phi_t + \beta(x,y)\nabla\phi \cdot n = 0,$$

with the initial condition $\phi(t=0)$ equal to $\mathcal{V}$ inside the domain Ω and zero elsewhere. Here n is defined everywhere in D by $\frac{\nabla\psi}{|\nabla\psi|}$ and β is zero or one corresponding to inside or outside of the domain Ω.

The mesh, used to solve the Hamilton-Jacobi equation, is coarser than the mesh used to solve the Helmholtz equation. We use an upwind scheme for solving the Hamilton-Jacobi equation [23, 25] and discretize Eq. (29) as follows

$$\frac{\psi_{ij}^{n+1} - \psi_{ij}^{n}}{\Delta t} + \left[\max\left(V_{ij},0\right)\nabla^{+} + \min\left(V_{ij},0\right)\nabla^{-}\right] = 0, \tag{31}$$

where

$$\begin{aligned}
\nabla^{+} &= \left[\max\left(D_{ij}^{-x},0\right)^2 + \min\left(D_{ij}^{+x},0\right)^2 + \max\left(D_{ij}^{-y},0\right)^2 + \min\left(D_{ij}^{+y},0\right)^2\right]^{1/2},\\
\nabla^{-} &= \left[\max\left(D_{ij}^{+x},0\right)^2 + \min\left(D_{ij}^{-x},0\right)^2 + \max\left(D_{ij}^{+y},0\right)^2 + \min\left(D_{ij}^{-y},0\right)^2\right]^{1/2},\\
D_{ij}^{-x} &= \frac{\psi^n(i,j) - \psi^n(i-1,j)}{\Delta x}, \quad D_{ij}^{+x} = \frac{\psi^n(i+1,j) - \psi^n(i,j)}{\Delta x},\\
D_{ij}^{-y} &= \frac{\psi^n(i,j) - \psi^n(i,j-1)}{\Delta y}, \quad D_{ij}^{+y} = \frac{\psi^n(i,j+1) - \psi^n(i,j)}{\Delta y},
\end{aligned}$$

and $\psi|_{t=0} = \psi_0$ is the signed distance function, defined in (30). Scheme (31) is stable under the CFL condition

$$\Delta t \leq \frac{\Delta x}{\max(|\mathcal{V}(x,y)|)\sqrt{2}} \tag{32}$$

with a space-step $\Delta x = \Delta y$.

6 Numerical experiments

For all numerical tests, presented below, we consider the rectangle $\overline{D} = [0,3]\times[0,1]$, and suppose that D always contains the domain Ω, on which we solve the Helmholtz equation. The boundaries Γ_N and Γ_D are fixed, as it is shown on Fig. 2, and Γ is the moving boundary inside of $\overline{G} = [\frac{3}{2},3]\times[0,1]$. The initial $\Omega_0 =]0,2[\times]0,1[$ has a flat boundary Γ_0 fixed at $x=2$. The characteristic lengths of Ω_0 are $\ell = 1$ and $L = 2\ell$.

The Helmholtz equation is considered with a wave number $k = \frac{\omega}{c_0}$, *i.e*,

$$\Delta u + k^2 u = -f,$$

where c_0 is the sound speed in the air. We take

$$f = 0, \quad g = \frac{1}{\sigma\sqrt{2\pi}}\exp\left(-\frac{(y-1/2)^2}{2\sigma^2}\right)$$

with $\sigma = 1$ in the Helmholtz boundary value problem. For the chosen σ, the smallest wavelength, excited by g, is $\lambda = \frac{\ell}{2}$. The parameter α in the Robin boundary condition depends on the value of the frequency ω. It is calculated for ISOREL, using a minimization of the difference between the solution of the problem with a volume dissipation (described by a damped wave equation) and the solution of the problem with the boundary dissipation for the flat shape of Γ (see Theorem 4 and Fig. 1). We solve the Helmholtz boundary value problem on the fine mesh with the size $h = \frac{\ell}{64}$, and we perform the level set approach for the optimization algorithm on the coarse mesh of the size $\kappa = 2h = \frac{\ell}{32}$ (in the aim of a penalization of too much complicated shapes of Γ). However, we notice that $\kappa \ll \lambda$.

Let us illustrate the stability properties of the optimization algorithm.

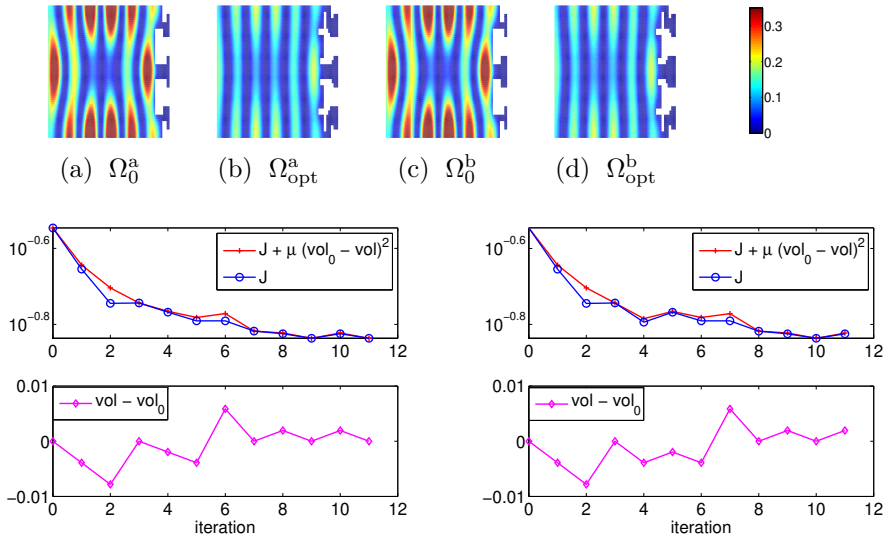

(a) Ω_0^{a} (b) $\Omega_{\mathrm{opt}}^{\mathrm{a}}$ (c) Ω_0^{b} (d) $\Omega_{\mathrm{opt}}^{\mathrm{b}}$

(f) Convergence starting by Ω_0^{a} (g) Convergence starting by Ω_0^{b}

Figure 3: The values of $|u|^2$ are presented on two initial and optimal domains for the fixed frequency $\omega_0 = 3170$. From the left to the right: the initial domain Ω_0^a and the corresponding optimal domain $\Omega_{\mathrm{opt}}^a = \Omega_{11}^a$, the initial domain Ω_0^b, taken in a small neighborhood of Ω_0^a, and the corresponding optimal domain $\Omega_{\mathrm{opt}}^b = \Omega_{10}^b$. We see that Ω_{opt}^a is in a small neighborhood of Ω_{opt}^b (the shapes of Γ^a and Γ^b are almost the same). The values of J are also almost the same: $J(\Omega_{\mathrm{opt}}^a)(\omega_0) \approx 0.1458$ and $J(\Omega_{\mathrm{opt}}^b)(\omega_0) \approx 0.1458$. As compared to the flat shape $\overline{\Omega}_0 = [0,2] \times [0,1]$, for which $J(\Omega_0)(\omega_0) = 4.286$, we have $J(\Omega_0)(\omega_0)/J(\Omega_{\mathrm{opt}}^a)(\omega_0) = 27.492$, hence the optimal shapes dissipate the energy 27.5 times better than the flat one. The bottom pictures show the convergence of the optimization algorithm for two cases of initial domain: for Ω_0^a in the left and for Ω_0^b in the right.

We fix the frequency $\omega_0 = 3170$, which is a local maximum of

$$J(\Omega)(\omega) = \int_\Omega |u|^2 \mathrm{d}x,$$

calculated for $\Omega_0 =]0,2[\times]0,1[$ in a range of frequencies, for instance, $\omega \in [3000, 6000]$. This time we chose $A = 1$ and $B = C = 0$ for the simulation of the acoustical energy.

If we start the optimization algorithm one time from $\Omega_0 = \Omega_0^a$ and the second time from $\Omega_0 = \Omega_0^b$, such that $d_H(\Omega_0^a, \Omega_0^b) < \varepsilon$ is mall enough, then the optimal shapes $\Omega_{\rm opt}^a$ and $\Omega_{\rm opt}^b$ are "almost the same", *i.e.* there exists $C > 0$, depending only on ε, such that the distance

$$d_H(\Omega_{\rm opt}^a, \Omega_{\rm opt}^b) < C(\varepsilon) d_H(\Omega_0^a, \Omega_0^b)$$

is also small enough. Hence, $|J(\Omega_{\rm opt}^a)(\omega_0) - J(\Omega_{\rm opt}^b)(\omega_0)| \ll 1$ is also small enough by the continuity of J as a function of the domain; see Fig. 3 for the numerical example.

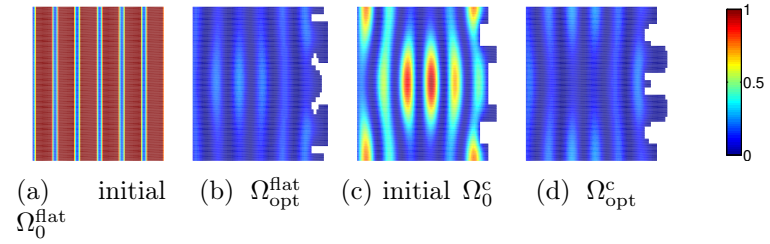

(a) initial $\Omega_0^{\rm flat}$ (b) $\Omega_{\rm opt}^{\rm flat}$ (c) initial $\Omega_0^{\rm c}$ (d) $\Omega_{\rm opt}^{\rm c}$

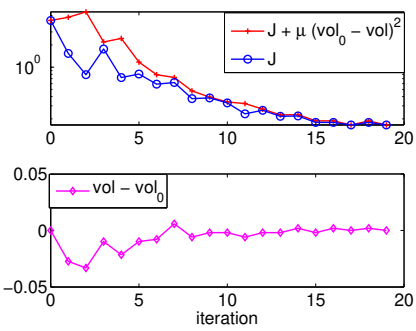

(f) Convergence starting by $\Omega_0^{\rm flat}$

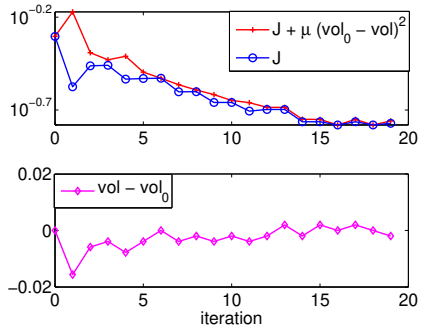

(g) Convergence starting by $\Omega_0^{\rm c}$

Figure 4: The values of $|u|^2$ are presented on two initial and optimal domains for the fixed frequency $\omega_0 = 3170$. From the left to the right: the initial domain $\Omega_0^{\rm flat}$ and the corresponding optimal domain $\Omega_{\rm opt}^{\rm flat}$, the initial domain Ω_0^c, significantly different to $\Omega_0^{\rm flat}$ and to $\Omega_{\rm opt}^{\rm flat}$, taken with characteristic geometric scales which are almost the same as for $\Omega_{\rm opt}^{\rm flat}$, and the corresponding optimal domain $\Omega_{\rm opt}^c$. We see that $\Omega_{\rm opt}^{\rm flat}$ is not in a small neighborhood of $\Omega_{\rm opt}^{\rm c}$ (the shapes of Γ^a and Γ^b are really different). But the values of J for $\omega_0 = 3170$ are also almost the same: $J(\Omega_{\rm opt}^{\rm flat}) = 0.1654$ and $J(\Omega_{\rm opt}^{\rm c}) = 0.1659$.

Let us also notice, that, as for the question of Mark Kac "Can one hear the shape of a drum?", we don't have the uniqueness of the optimal shape Γ, since different shapes can have the same spectrum and be identically efficient in the dissipation of the energy in the fixed range of frequency. Fig. 4 illustrates the case, when the initial shape $\Omega_0 = \Omega_0^c$ is not in a small neighborhood of $\Omega_{\rm opt}^a$ and the characteristic geometric scales of Ω_0^c are almost the same as for $\Omega_{\rm opt}^a$. For this choice of Ω_0^c we obtain that $\Omega_{\rm opt}^c$ is not in a small neighborhood of $\Omega_{\rm opt}^{\rm flat}$, but we still have $|J(\Omega_{\rm opt}^c)(\omega_0) - J(\Omega_{\rm opt}^a)(\omega_0)| \ll 1$. Moreover,

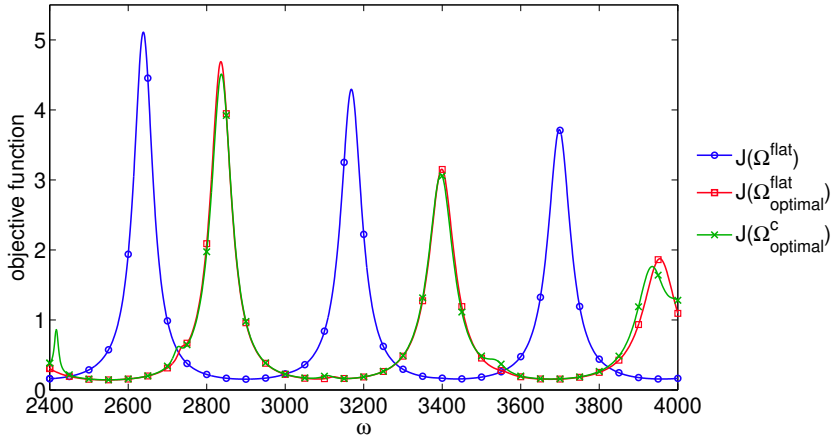

Figure 5: The objective function J as a function of ω for the flat shape Ω_0, for the optimal shape $\Omega^{\rm flat}_{\rm opt}$ (see Fig. 4) and for the optimal shape $\Omega^{c}_{\rm opt}$ (see Fig. 4).

Fig. 5 shows, that the values of the functional $|J(\Omega^c_{\rm opt})(\omega) - J(\Omega^a_{\rm opt})(\omega)| \ll 1$ are almost the same for all ω in a rather large neighborhood of ω_0.

Fig. 5 also shows that the minimization process for one given frequency (here $\omega_0 = 3170$, corresponding to the middle peak of $J(\Omega^{\rm flat})$) is very efficient, but it creates peaks at other frequencies, and so, we need a strategy to find the most efficient shape, able to dissipate the acoustical energy in a large range of frequencies.

7 Conclusion

We showed that the problem of finding an optimal shape for the Helmholtz problem with a dissipative boundary has at least one solution. We developed an algorithm and numerical methods allowing to calculate optimal shapes numerically. Our numerical results show the necessity of the next step, which is to consider the question of how to find the simplest and most efficient shape of a noise absorbing wall to dissipate the energy of a sound wave in a range of frequencies. It is the subject of Part II [18].

A Approximation of the damping parameter α in the Robin boundary condition by a model with dissipation in the volume

Theorem 4 *Let $\Omega =]-L, L[\times]-\ell, \ell[$ be a domain with a simply connected sub-domain Ω_0, whose boundaries are $]-L, 0[\times \{\ell\}$, $\{-L\} \times]-\ell, \ell[$, $]-L, 0[\times \{-\ell\}$ and another boundary, denoted by Γ, which is the straight line starting in $(0, -\ell)$ and ending in $(0, \ell)$. In addition let Ω_1 be the supplementary domain of Ω_0 in Ω, so that Γ is the common boundary of Ω_0 and Ω_1. The length L is supposed to be large enough.*

Let the original problem (the frequency version of the wave damped problem (1)) be

$$-\nabla \cdot (\mu_0 \nabla u_0) - \omega^2 \xi_0 u_0 = 0 \quad in\ \Omega_0, \tag{33}$$

$$-\nabla \cdot (\mu_1 \nabla u_1) - \omega^2 \tilde{\xi}_1 u_1 = 0 \quad in\ \Omega_1, \tag{34}$$

with

$$\tilde{\xi}_1 = \xi_1 \left(1 + \frac{ai}{\xi_1 \omega}\right),$$

together with boundary conditions on Γ

$$u_0 = u_1 \quad and \quad \mu_0 \nabla u_0 \cdot n = \mu_1 \nabla u_1 \cdot n, \tag{35}$$

and the condition on the left boundary

$$u_0(-L, y) = g(y), \tag{36}$$

and some other boundary conditions. Let the modified problem be

$$-\nabla \cdot (\mu_0 \nabla u_2) - \omega^2 \xi_0 u_2 = 0 \quad in\ \Omega_0 \tag{37}$$

with boundary absorption condition on Γ

$$\mu_0 \nabla u_2 \cdot n + \alpha u_2 = 0 \tag{38}$$

and the condition on the left boundary

$$u_2(-L, y) = g(y). \tag{39}$$

Let u_0 , u_1 , u_2 *and* g *be decomposed into Fourier modes in the* y *direction, denoting by* k *the associated wave number. Then the complex parameter* α *, minimizing the following expression*

$$A||u_0 - u_2||^2_{L^2(\Omega_0)} + B||\nabla(u_0 - u_2)||^2_{L^2(\Omega_0)}$$

can be found from the minimization of the error function

$$e(\alpha) := \sum_{k=\frac{n\pi}{L}, n\in\mathbb{Z}} e_k(\alpha),$$

where e_k *are given by*

$$\begin{aligned} e_k(\alpha) = (A + B|k|^2) \Bigg(& \frac{1}{2\lambda_0} \left\{ |\chi|^2 \left[1 - \exp(-2\lambda_0 L)\right] \right. \\ & \left. + |\eta|^2 \left[\exp(2\lambda_0 L) - 1\right] \right\} + 2L \mathrm{Re}\left(\chi \bar{\eta}\right) \Bigg) \\ & + B\frac{\lambda_0}{2} \left\{ |\chi|^2 \left[1 - \exp(-2\lambda_0 L)\right] + |\eta|^2 \left[\exp(2\lambda_0 L) - 1\right] \right\} - 2B\lambda_0^2 L \mathrm{Re}\left(\chi \bar{\eta}\right) \end{aligned}$$

if $k^2 \geq \frac{\xi_0}{\mu_0}\omega^2$ *or*

$$\begin{aligned} & e_k(\alpha) = (A + B|k|^2) \left(L(|\chi|^2 + |\eta|^2) + \frac{i}{\lambda_0} \mathrm{Im}\left\{ \chi \bar{\eta} \left[1 - \exp(-2\lambda_0 L)\right] \right\} \right) \\ & + BL|\lambda_0|^2 \left(|\chi|^2 + |\eta|^2 \right) + iB\lambda_0 \mathrm{Im}\left\{ \chi \bar{\eta} \left[1 - \exp(-2\lambda_0 L)\right] \right\} \end{aligned}$$

if $k^2 < \frac{\xi_0}{\mu_0}\omega^2$ *, in which*

$$f(x) = (\lambda_0\mu_0 - x)\exp(-\lambda_0 L) + (\lambda_0\mu_0 + x)\exp(\lambda_0 L),$$
$$\chi(k,\alpha) = g_k\left(\frac{\lambda_0\mu_0 - \lambda_1\mu_1}{f(\lambda_1\mu_1)} - \frac{\lambda_0\mu_0 - \alpha}{f(\alpha)}\right),$$
$$\eta(k,\alpha) = g_k\left(\frac{\lambda_0\mu_0 + \lambda_1\mu_1}{f(\lambda_1\mu_1)} - \frac{\lambda_0\mu_0 + \alpha}{f(\alpha)}\right),$$

where

$$\begin{cases} \lambda_0 = \sqrt{k^2 - \frac{\xi_0}{\mu_0}\omega^2} & \text{if} \quad k^2 \geq \frac{\xi_0}{\mu_0}\omega^2, \\ \lambda_0 = i\sqrt{\frac{\xi_0}{\mu_0}\omega^2 - k^2} & \text{if} \quad k^2 \leq \frac{\xi_0}{\mu_0}\omega^2. \end{cases} \tag{40}$$

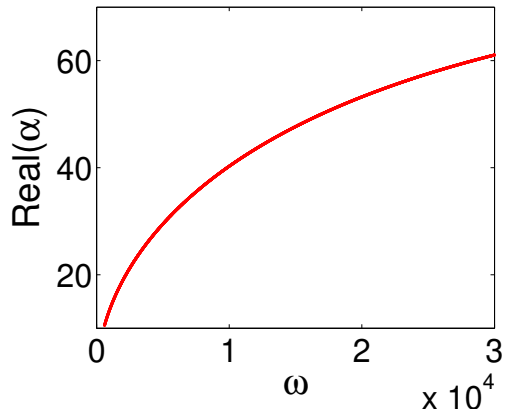

(a) Re(α)

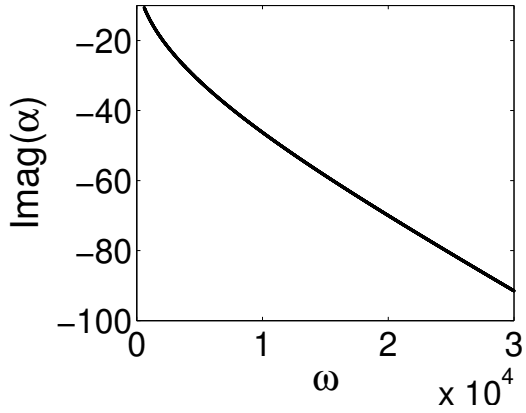

(b) Im(α)

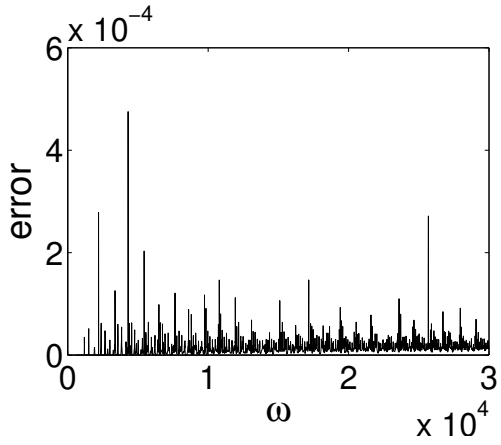

(c) error

Figure 6: The real (top left) and imaginary (top right) parts of α and the sum of the errors $e_{\Delta x}$ (in the bottom) as function of frequencies $\omega \in [600, 30000]$ calculated for the ISOREL porous material.

Since the minimization will be done numerically and since the sequence $(z, -z, z - z, \cdots) = z(\exp(i(j\Delta x)/\Delta x))$ is the highest frequency mode that can be reached on a

grid of size Δx, then, in practice, the sum may be truncated to

$$e_{\Delta x}(\alpha) := \sum_{k=\frac{n\pi}{L}, n\in\mathbb{Z}, -\frac{L}{\Delta x}\leq n\leq \frac{L}{\Delta x}} e_k(\alpha).$$

For the equations (33)–(34), we use the same coefficients as for problem (1) and take the values corresponding to a porous medium, called ISOREL, using in the building isolation. More precisely we assume: $\phi = 0.7$, $\gamma_p = 1.4$, $\sigma = 142300N.m^{-4}.s$, $\rho_0 = 1.2kg/m^3$, $\alpha_h = 1.15$, $c_0 = 340m.s^{-1}$. Using the function $fminsearch$ (in Matlab), we find the value of α presented in Fig. A.

Remark 2 *Fig. A allows us to compare the difference between two considered time-dependent models for the damping in the volume and for the damping on the boundary. We see that* $\mathrm{Re}(\alpha)$ *is not a constant in general, but for* $\omega \to +\infty$ $\mathrm{Im}(\alpha)$ *is a linear function of* ω*. In this sense, the damping properties of two models are almost the same, but the reflection is more accurately considered by the damping wave equation in the volume.*

B Proof of Theorem 4

Proof. First of all,

$$e(\alpha) := A||u_0 - u_2||^2_{L^2(\Omega_0)} + B||\nabla(u_0 - u_2)||^2_{L^2(\Omega_0)}$$

can be decomposed as a sum of $e_k(\alpha)$

$$e(\alpha) := \sum_{k=\frac{n\pi}{L}, n\in\mathbb{Z}} e_k(\alpha),$$

with

$$e_k(\alpha) = A||u_{0,k} - u_{2,k}||^2_{L^2(]-L,0[)} + B||\nabla(u_{0,k} - u_{2,k})||^2_{L^2(]-L,0[)},$$

where we have decomposed decomposed u_0, u_1 and u_2 into modes in the y direction, denoting by k the associated wave number.

The mode $u_{0,k}$ solves

$$\partial_{xx} u_{0,k} - \left(k^2 - \frac{\xi_0}{\mu_0}\omega^2\right) u_{0,k} = 0,$$

and thus

$$u_{0,k}(x) = A_0 \exp(\lambda_0 x) + B_0 \exp(-\lambda_0 x), \tag{41}$$

where λ_0 is given in Eq. (40).

The mode $u_{1,k}$ solves

$$\partial_{xx} u_{1,k} - \left(k^2 - \frac{\tilde{\xi}_1}{\mu_1}\omega^2\right) u_{1,k} = 0,$$

and thus

$$u_{1,k}(x) = A_1 \exp(\lambda_1 x) + B_1 \exp(-\lambda_1 x), \tag{42}$$

where

$$\lambda_1^2 = k^2 - \left(1 + \frac{ai}{\xi_1 \omega}\right) \frac{\xi_1}{\mu_1} \omega^2,$$

so that

$$\lambda_1 = \frac{1}{\sqrt{2}} \sqrt{k^2 - \frac{\xi_1}{\mu_1}\omega^2 + \sqrt{\left(k^2 - \frac{\xi_1}{\mu_1}\omega^2\right)^2 + \left(\frac{a\omega}{\mu_1}\right)^2}}$$
$$- \frac{i}{\sqrt{2}} \sqrt{\frac{\xi_1}{\mu_1}\omega^2 - k^2 + \sqrt{\left(k^2 - \frac{\xi_1}{\mu_1}\omega^2\right)^2 + \left(\frac{a\omega}{\mu_1}\right)^2}}.$$

For large L, since $Re(\lambda_1) > 0$, the value of A_1 tend to 0, so that we may neglect the first contribution in the right-hand side of (42). Consequently we consider the expression

$$u_{1,k}(x) = B_1 \exp(-\lambda_1 x). \tag{43}$$

Continuity conditions (35) and expressions (41) and (43) imply the following relations

$$A_0 + B_0 = B_1 \quad , \quad \mu_0 \lambda_0 (A_0 - B_0) = -\mu_1 \lambda_1 B_1,$$

from which we infer that

$$B_0 = \frac{\lambda_0 \mu_0 + \lambda_1 \mu_1}{\lambda_0 \mu_0 - \lambda_1 \mu_1} A_0,$$

and thus

$$u_{0,k}(x) = A_0 \left[\exp(\lambda_0 x) + \frac{\lambda_0 \mu_0 + \lambda_1 \mu_1}{\lambda_0 \mu_0 - \lambda_1 \mu_1} \exp(-\lambda_0 x)\right].$$

The decomposition of the boundary condition (36) into Fourier modes implies that $u_{0,k}(-L) = g_k$, which gives the final expression

$$u_{0,k}(x) = g_k \frac{[(\lambda_0 \mu_0 - \lambda_1 \mu_1) \exp(\lambda_0 x) + (\lambda_0 \mu_0 + \lambda_1 \mu_1) \exp(-\lambda_0 x)]}{[(\lambda_0 \mu_0 - \lambda_1 \mu_1) \exp(-\lambda_0 L) + (\lambda_0 \mu_0 + \lambda_1 \mu_1) \exp(\lambda_0 L)]}. \tag{44}$$

Let us now turn to the expression of $u_{2,k}$. Since the equation (37) is the same as that verified by $u_{0,k}$, both solutions have the same general form:

$$u_{2,k}(x) = A_2 \exp(\lambda_0 x) + B_2 \exp(-\lambda_0 x).$$

The Robin boundary condition (38) on Γ implies that

$$\mu_0 \lambda_0 (A_2 - B_2) + \alpha (A_2 + B_2) = 0,$$

which means that

$$u_{2,k}(x) = A_2 \left[\exp(\lambda_0 x) + \frac{\lambda_0 \mu_0 + \alpha}{\lambda_0 \mu_0 - \alpha} \exp(-\lambda_0 x)\right].$$

Application of the boundary condition (39) implies the final expression

$$u_{2,k}(x) = g_k \frac{[(\lambda_0\mu_0 - \alpha)\exp(\lambda_0 x) + (\lambda_0\mu_0 + \alpha)\exp(-\lambda_0 x)]}{[(\lambda_0\mu_0 - \alpha)\exp(-\lambda_0 L) + (\lambda_0\mu_0 + \alpha)\exp(\lambda_0 L)]}. \tag{45}$$

Using (44) and (45), we have that

$$(u_{0,k} - u_{2,k})(x) = \chi(k,\alpha)\exp(\lambda_0 x) + \eta(k,\alpha)\exp(-\lambda_0 x), \tag{46}$$

where the coefficients χ and η are computed from (44) and (45). In order to compute the L^2 norm of this expression, we must first compute the square of its modulus (by $\bar{\eta}$ is denoted the complex conjugate of η):

$$|u_{0,k} - u_{2,k}|^2(x) = |\chi|^2|\exp(\lambda_0 x)|^2 + |\eta|^2|\exp(-\lambda_0 x)|^2 + 2\mathrm{Re}\left(\chi\bar{\eta}\exp(\lambda_0 x)\overline{\exp(-\lambda_0 x)}\right).$$

Note that, according to the values of k, the expression above may be simplified into

$$|u_{0,k} - u_{2,k}|^2(x) = |\chi|^2\exp(2\lambda_0 x) + |\eta|^2\exp(-2\lambda_0 x) + 2\mathrm{Re}\left(\chi\bar{\eta}\right),$$

if $k^2 \geq \frac{\xi_0}{\mu_0}\omega^2$, or

$$|u_{0,k} - u_{2,k}|^2(x) = |\chi|^2 + |\eta|^2 + 2\mathrm{Re}\left(\chi\bar{\eta}\exp(2\lambda_0 x)\right),$$

if $k^2 < \frac{\xi_0}{\mu_0}\omega^2$. Thus, we have for $k^2 \geq \frac{\xi_0}{\mu_0}\omega^2$

$$\int_{-L}^{0} |u_{0,k} - u_{2,k}|^2(x)\mathrm{d}x = \frac{1}{2\lambda_0}\left\{|\chi|^2\left[1 - \exp(-2\lambda_0 L)\right] + |\eta|^2\left[\exp(2\lambda_0 L) - 1\right]\right\} + 2L\mathrm{Re}\left(\chi\bar{\eta}\right)$$

or, for $k^2 < \frac{\xi_0}{\mu_0}\omega^2$,

$$\int_{-L}^{0} |u_{0,k} - u_{2,k}|^2(x)\mathrm{d}x = L(|\chi|^2 + |\eta|^2) + \frac{i}{\lambda_0}\mathrm{Im}\left\{\chi\bar{\eta}\left[1 - \exp(-2\lambda_0 L)\right]\right\}.$$

Now, we also have to compute the L^2 norm of the gradient of $(u_{0,k} - u_{2,k})$. Noting that

$$\nabla(u_{0,k} - u_{2,k}) = \begin{pmatrix} \partial_x(u_{0,k} - u_{2,k}) \\ ik(u_{0,k} - u_{2,k}) \end{pmatrix},$$

it holds that

$$|\nabla(u_{0,k} - u_{2,k})|^2 = |k|^2|u_{0,k} - u_{2,k}|^2 + |\partial_x(u_{0,k} - u_{2,k})|^2.$$

With the expression (46), it follows that

$$|\partial_x(u_{0,k} - u_{2,k})|^2 = |\lambda_0|^2\left[|\chi|^2\exp(2\lambda_0 x) + |\eta|^2\exp(-2\lambda_0 x) - 2\mathrm{Re}\left(\chi\bar{\eta}\right)\right],$$

if $k^2 \geq \frac{\xi_0}{\mu_0}\omega^2$, or

$$|\partial_x(u_{0,k} - u_{2,k})|^2 = |\lambda_0|^2\left[|\chi|^2 + |\eta|^2 - 2\mathrm{Re}\left(\chi\bar{\eta}\exp(2\lambda_0 x)\right)\right],$$

if $k^2 < \frac{\xi_0}{\mu_0}\omega^2$, and thus

$$\int_{-L}^{0} |\partial_x(u_{0,k} - u_{2,k})|^2(x)\mathrm{d}x = \frac{\lambda_0}{2}\left\{|\chi|^2\left[1-\exp(-2\lambda_0 L)\right] + |\eta|^2\left[\exp(2\lambda_0 L) - 1\right]\right\} - 2\lambda_0^2 L\mathrm{Re}\left(\chi\bar{\eta}\right),$$

if $k^2 \geq \frac{\xi_0}{\mu_0}\omega^2$, or, if $k^2 < \frac{\xi_0}{\mu_0}\omega^2$,

$$\int_{-L}^{0} |\partial_x(u_{0,k} - u_{2,k})|^2(x)\mathrm{d}x = L|\lambda_0|^2\left(|\chi|^2 + |\eta|^2\right) + i\lambda_0\mathrm{Im}\left\{\chi\bar{\eta}\left[1-\exp(-2\lambda_0 L)\right]\right\}.$$

Therefore, we can find α as the solution of the mentioned minimization problem. □

Acknowledgment

The author are also very grateful to T. Kako and B. Sapoval for their comments and discussions during this long term trend.

References

[1] K. Abe, T. Fujiu, and K. Koro, *A BE-based shape optimization method enhanced by topological derivative for sound scattering problems*, Engineering Analysis with Boundary Elements, 34 (2010), pp. 1082–1091, https://doi.org/10.1016/j.enganabound.2010.06.017.

[2] Y. Achdou and O. Pironneau, *Optimization of a photocell*, Optimal Control Applications and Methods, 12 (1991), pp. 221–246, https://doi.org/10.1002/oca.4660120403.

[3] G. Allaire, *Conception optimale de structures*, 58 Mathématiques et Applications, Springer, 2007.

[4] H. Antil, S. Hardesty, and M. Heinkenschloss, *Shape Optimization of Shell Structure Acoustics*, SIAM Journal on Control and Optimization, 55 (2017), pp. 1347–1376, https://doi.org/10.1137/16{M}1070633.

[5] M. Asch and G. Lebeau, *The Spectrum of the Damped Wave Operator for a Bounded Domain in* $\mathbb{R}^2$, Experimental Mathematics, 12 (2003), pp. 227–241, https://doi.org/10.1080/10586458.2003.10504494.

[6] C. Bardos and J. Rauch, *Variational algorithms for the Helmholtz equation using time evolution and artificial boundaries*, Asymptotic Analysis, 9 (1994), pp. 101–117.

[7] D. Bucur, D. Mazzoleni, A. Pratelli, and B. Velichkov, *Lipschitz Regularity of the Eigenfunctions on Optimal Domains*, Arch Rational Mech Anal, 216 (2014), pp. 117–151, https://doi.org/10.1007/s00205-014-0801-6.

[8] Y. Cao and D. Stanescu, *Shape optimization for noise radiation problems*, Computers & Mathematics with Applications, 44 (2002), pp. 1527–1537, https://doi.org/10.1016/{S}0898-1221(02)00276-6.

[9] S. Cox and E. Zuazua, *The rate at which energy decays in a damped string*, Communications in Partial Differential Equations, 19 (1994), pp. 213–243, https://doi.org/10.1080/03605309408821015.

[10] D. Duhamel, *Calcul de murs antibruit et control actif du son*, PhD thesis, 1998.

[11] D. Duhamel, *Shape optimization of noise barriers using genetic algorithms*, Journal of Sound and Vibration, 297 (2006), pp. 432–443, https://doi.org/10.1016/j.jsv.2006.04.004.

[12] L. C. Evans, *Partial Differential Equations*, American Math Society, 2010.

[13] B. Farhadinia, *An Optimal Shape Design Problem for Fan Noise Reduction*, JSEA, 03 (2010), pp. 610–613, https://doi.org/10.4236/jsea.2010.36071.

[14] M. J. Gander, L. Halpern, and F. Magoulès, *An optimized Schwarz method with two-sided Robin transmission conditions for the Helmholtz equation*, International Journal for Numerical Methods in Fluids, 55 (2007), pp. 163–175, https://doi.org/10.1002/fld.1433.

[15] D. Guicking, *On the invention of active noise control by Paul Lueg*, The Journal of the Acoustical Society of America, 87 (1990), p. 2251, https://doi.org/10.1121/1.399195.

[16] J.-F. Hamet and M. Berengier, *Acoustical characteristics of porous pavements: a new phenomenological model*, Internoise 93,Louvain, Belgique, (1993), pp. 641–646.

[17] A. Henrot and M. Pierre, *Variation et optimization de formes. Une analyse géométrique*, Springer, 2005.

[18] F. Magoulès, T. P. K. Nguyen, P. Omnès, and A. Rozanova Pierrat, *Optimal absorption of acoustical waves by a boundary, Part 2*, Submitted, (2017).

[19] B. Mohammadi and O. Pironneau, *Applied shape optimization for fluids*, Oxford University Press, 2010.

[20] A. Münch, *Optimal Internal Dissipation of a Damped Wave Equation Using a Topological Approach*, International Journal of Applied Mathematics and Computer Science, 19 (2009), https://doi.org/10.2478/v10006-009-0002-x.

[21] A. Münch, P. Pedregal, and F. Periago, *Optimal design of the damping set for the stabilization of the wave equation*, Journal of Differential Equations, 231 (2006), pp. 331–358, https://doi.org/10.1016/j.jde.2006.06.009.

[22] F. Murat and J. Simon, *Optimal Design*, Optimization Techniques Modeling and Optimization in the Service of Man Part 2, Lecture Notes in Computer Science, 41 (2005), pp. 52–62.

[23] S. Osher and R. Fedkiw, *Level set method and dynamic implicit surfaces*, vol. 153, Applied Mathematical Sciences, Springer, 2003.

[24] S. Osher and J.-A. Sethian, *Fronts propagating with curvature dependent speed: algorithm based on Hamilton-Jacobi formulations*, J. Comp. Phys, 79 (1988).

[25] J. Sethian and R. Fedkiw, *Level set method and fast marching methods*, Cambridge Univerity Press, 1999.

Optimal absorption of acoustical waves by a boundary. Part II

Frédéric Magoulès[*], Thi Phuong Kieu Nguyen[*],
Pascal Omnes[†], Anna Rozanova-Pierrat[*]

January 19, 2018

[1] [2]

Abstract

In the aim to find the simplest and most efficient shape of a noise absorbing wall to dissipate the energy of a sound wave, we consider a frequency model (the Helmholtz equation) with a damping on the boundary. Once the well-posedness result is proved in the class of bounded n-sets (for instance, locally uniform domains with a d-set boundary, containing self-similar fractals or Lipschitz domains as examples), the shape optimization problem of minimizing the acoustical energy for a large range of frequencies is considered. Introducing the notion of ε-optimal shapes, we prove that for the energy dissipation on a finite range of frequencies, the most efficient shapes belong to a class of multiscale Lipschitz boundaries, and for an infinite frequency range, belong to a class of fractals. The theory is illustrated by numerical results.

1 Introduction

This is the second part of studies of the question about the form of the simplest and most efficient shape of a noise absorbing wall to dissipate the energy of a sound wave. Knowing from Part I [23] the existence of an optimal shape for a fixed frequency of a two-dimensional shape optimization problem for a Helmholtz equation with a damping on the boundary, we are interested in the same question for a frequency range.

We start in Section 2 by the well-posedness results of the Helmholtz model introduced in Part I [23] with dissipative boundary Robin conditions in a large class of bounded domains (see Theorems 1, 2 and Theorem 3), containing Lipschitz domains and von Koch fractals as two particular cases.

In Section 3, to obtain an efficient wall shape for a large range of frequencies, we define ε-optimal shapes. Knowing empirically that for the efficient energy dissipation of

[1] Laboratoire de Mathématiques et Informatique pour la Complexité et les Systèmes, CentralSupélec, Université Paris-Saclay, 3 rue Joliot Curie, F-91192 Gif-sur-Yvette, France.

[2] CEA, DEN, DANS, DM2S, STMF, F-91191 Gif sur Yvette Cedex, France and Université Paris 13, Sorbonne Paris Cité, LAGA, CNRS (UMR 7539), 99 Avenue J.-B. Clément F-93430, Villetaneuse Cedex, France.

an acoustic wave, its wavelength λ must be related with a geometric scale of the wall, we confirm this fact numerically by calculating the impact of the different geometric scales on the energy dissipation in time (see Fig. 3, which confirms a guess that the wall length scale must be of the order of $\lambda/2$). The optimization algorithm developed in Part I [23] confirms that the optimal shape has its largest scale length of the order of $\lambda/2$ (see Subsection 4.1 and Fig. 5).

Moreover, using the fact that a wave with a wavelength λ does not fit into a shape that has a characteristic scale much smaller than its wavelength (smaller than $\lambda/2$), we prove in Section 3 that it is not possible to obtain the "most efficient" shape for energy dissipation (an ε-optimal shape with a minimal $\varepsilon > 0$) for all frequencies without different geometric scales. Actually, for an infinite frequency range, such efficient shapes are fractals. In Section 4.2 we obtain numerically an ε-optimal shape for a large range of frequencies. This shape is multiscale, and we show that if we keep only the largest scale, the new shape has the same good dissipation properties as the optimal one in the low frequencies corresponding to the chosen scale length, but is no more efficient in higher frequencies, for which the deleted geometry scales where important.

2 Well-posedness of the Helmholtz equation with a dissipative Robin boundary condition on a d-set

We extend the well-posedness result of Theorem 2.2 of Part I [23] for the frequency model to a more general class of boundaries, named Ahlfors d-regular sets or simply d-sets [18], using the functional analysis on (ε, δ)-domains [17, 18, 26], also called locally uniform domains [16]. Let us define the main notions [2].

Definition 1 (Ahlfors d-regular set or d-set [18, 26, 19]) *Let F be a Borel subset of $\mathbb{R}^n$ and m_d be the d-dimensional Hausdorff measure, $0 < d \leq n$, $d \in \mathbb{R}$. The set F is called a d-set, if there exist positive constants c_1, $c_2 > 0$,*

$$c_1 r^d \leq m_d(F \cap B_r(x)) \leq c_2 r^d, \quad \text{for } \forall\, x \in F,\ 0 < r \leq 1,$$

where $B_r(x) \subset \mathbb{R}^n$ denotes the Euclidean ball centered at x and of radius r.

Definition 2 ((ε, δ)-domain [17, 18, 26]) *An open connected subset Ω of $\mathbb{R}^n$ is an (ε, δ)-domain, $\varepsilon > 0$, $0 < \delta \leq \infty$, if whenever $(x, y) \in \Omega^2$ and $|x - y| < \delta$, there is a rectifiable arc $\gamma \subset \Omega$ with length $\ell(\gamma)$ joining x to y and satisfying*

1. $\ell(\gamma) \leq \frac{|x-y|}{\varepsilon}$ *and*
2. $d(z, \partial\Omega) \geq \varepsilon |x - z| \frac{|y-z|}{|x-y|}$ *for $z \in \gamma$.*

It is known [26] that all (ε, δ) domains in $\mathbb{R}^n$ are n-sets (d-set with $d = n$):

$$\exists c > 0 \quad \forall x \in \overline{\Omega},\ \forall r \in]0, \delta[\cap]0, 1] \quad \mu(B_r(x) \cap \Omega) \geq C\mu(B_r(x)) = cr^n,$$

where $\mu(A)$ denotes the Lebesgue measure of a set A. This property is also called the measure density condition [12]. Let us notice that an n-set Ω cannot be "thin" close to its

boundary $\partial\Omega$. In the same time [26], if Ω is an (ε,δ)-domain and $\partial\Omega$ is a d-set ($d<n$), then $\overline{\Omega}=\Omega\cup\partial\Omega$ is an n-set. In particular, a Lipschitz domain Ω is an (ε,δ)-domain and also an n-set [26]. But not every n-set is an (ε,δ)-domain: adding an in-going cusp to an (ε,δ)-domain we obtain an n-set which is not an (ε,δ)-domain anymore. Self-similar fractals (e.g., von Koch's snowflake domain) are examples of (ε,∞)-domains with a d-set boundary [8, 26] for $d>n-1$.

To extend the usual variational formulations introduced in Refs. [5, 11] to d-set type fractal boundaries, we use, as in Ref. [2], the existence of the d-dimensional Hausdorff measure m_d on $\partial\Omega$ (see Definition 1) and a generalization of the usual trace theorem and the Green formula in the sense of the Besov space $B^{2,2}_{\beta}(\partial\Omega)$ with $\beta=1-\frac{n-d}{2}>0$ (for the definition of the Besov spaces on d-sets see Ref. [18] p.135 and Ref. [26] or Appendix in Ref. [4]). Note that for $d=n-1$, one has $\beta=\frac{1}{2}$ and $B^{2,2}_{\frac{1}{2}}(\partial\Omega)=H^{\frac{1}{2}}(\partial\Omega)$.

Let us start with the generalization of the notion of the trace:

Definition 3 (Trace operator) *For an arbitrary open set Ω of $\mathbb{R}^n$, the trace operator* Tr *is defined [18, 6, 21] for $u\in L^1_{loc}(\Omega)$ by*

$$\mathrm{Tr}\,u(x)=\lim_{r\to 0}\frac{1}{m(\Omega\cap U_r(x))}\int_{\Omega\cap U_r(x)}u(y)\mathrm{d}y,$$

where m denotes the Lebesgue measure. The trace operator Tr *is considered for all $x\in\overline{\Omega}$ for which the limit exists.*

Henceforth, the boundary $\partial\Omega$ is a d-set endowed with the d-dimensional Hausdorff measure, and $L_2(\partial\Omega)$ is defined with respect to this measure as well. Hence, the following Theorem (see Ref. [2] Section 2) generalizes the classical results [22, 24] for the Lipschitz boundaries $\partial\Omega$:

Theorem 1 *Let Ω be an admissible in the sense of Ref. [2] domain in $\mathbb{R}^n$, i.e. Ω is an n-set, such that its boundary $\partial\Omega$ is a compact d-set, $n-2<d<n$, and the norms $\|f\|_{H^1(\Omega)}$ and $\|f\|_{C^1_2(\Omega)}=\|f\|_{L_2(\Omega)}+\|f^{\sharp}_{1,\Omega}\|_{L_2(\Omega)}$ with*

$$f^{\sharp}_{1,\Omega}(x)=\sup_{r>0}r^{-1}\inf_{c\in\mathbb{R}}\frac{1}{\mu(B_r(x))}\int_{B_r(x)\cap\Omega}|f(y)-c|\mathrm{d}y$$

are equivalent on $H^1(\Omega)$. Then,

1. *$H^1(\Omega)$ is compactly embedded in $L^{loc}_2(\Omega)$ or in $L_2(\Omega)$ if Ω is bounded;*
2. *$\mathrm{Tr}_{\Omega}:H^1(\mathbb{R}^n)\to H^1(\Omega)$ is a linear continuous and surjective operator with linear bounded inverse (the extension operator $E_{\Omega}:H^1(\Omega)\to H^1(\mathbb{R}^n)$);*
3. *for $\beta=1-(n-d)/2>0$ the operators $\mathrm{Tr}:H^1(\mathbb{R}^n)\to L_2(\partial\Omega)$, and $\mathrm{Tr}_{\partial\Omega}:H^1(\Omega)\to L_2(\partial\Omega)$ are linear compact operators with dense image $\mathrm{Im}(\mathrm{Tr})=\mathrm{Im}(\mathrm{Tr}_{\partial\Omega})=B^{2,2}_{\beta}(\partial\Omega)$ and with linear bounded right inverse (the extension operators) $E:B^{2,2}_{\beta}(\partial\Omega)\to H^1(\mathbb{R}^n)$ and $E_{\partial\Omega}:B^{2,2}_{\beta}(\partial\Omega)\to H^1(\Omega)$;*

4. *the Green formula holds (see also Refs. [21, 7] for the von Koch case in* $\mathbb{R}^2$ *) for all* u *and* v *from* $H^1(\Omega)$ *with* $\Delta u \in L_2(\Omega)$ *:*

$$\int_\Omega v\Delta u\mathrm{d}x + \int_\Omega \nabla v.\nabla u\mathrm{d}x = \langle \frac{\partial u}{\partial n}, \mathrm{Tr}v\rangle_{((B^{2,2}_\beta(\partial\Omega))',B^{2,2}_\beta(\partial\Omega))}, \tag{1}$$

where the dual Besov space $(B^{2,2}_\beta(\partial\Omega))' = B^{2,2}_{-\beta}(\partial\Omega)$ *is introduced in Ref. [19].*

Remark 1 *Theorem 1 is a particular case of the results proven in Ref. [2], thanks to Refs. [12, 17, 18, 19, 26].*

We also notice that in the framework of the Sobolev space H^1 *and the Besov spaces* $B^{2,2}_\beta$ *with* $\beta < 1$*, as here, we do not need to impose Markov's local inequality on* $\partial\Omega$ *(see Ref. [18] p.39), as it is trivially satisfied (see Ref. [20] p. 198). If we work with more regular spaces,* H^k *with* $k \geq 2$*,* $k \in \mathbb{N}^*$*, we need to add the assumption that* $\partial\Omega$ *preserves Markov's local inequality: for every fixed* $k \in \mathbb{N}^*$*, there exists a constant* $c = c(V, n, k) > 0$*, such that*

$$\max_{\partial\Omega\cap\overline{B_r(x)}} |\nabla P| \leq \frac{c}{r} \max_{\partial\Omega\cap\overline{B_r(x)}} |P|$$

for all polynomials $P \in \mathcal{P}_k$ *and all closed balls* $\overline{B_r(x)}$*,* $x \in \partial\Omega$ *and* $0 < r \leq 1$*.*

For $n = 2$*, if* Ω *is a bounded connected domain, then, thanks to [17] and [12] (see also Proposition 1 in Ref. [2]),* Ω *is an* (ε, δ)*-domain.*

In this framework we prove the following theorem

Theorem 2 *Let* Ω *be a bounded domain in* $\mathbb{R}^n$ *satisfying the conditions of Theorem 1 (for instance an* (ε, δ)*-domain) with a closed* d*-set boundary* $\partial\Omega = \Gamma_D \cup \Gamma_N \cup \Gamma$*,* $n - 2 < d < n$*. By* m_d *is denoted the* d*–dimensional Hausdorff measure on* $\partial\Omega$ *(see Definition 1). Let in addition* $\mathrm{Re}(\alpha(x)) > 0$*,* $\mathrm{Im}(\alpha(x)) < 0$ *be continuous functions on* Γ *and*

$$V(\Omega) := \left\{u \in H^1(\Omega) |\ \mathrm{Tr}u|_{\Gamma_D} = 0\right\}$$

be the space with the norm $\|u\|_{V(\Omega)} = \sqrt{(u,u)_{V(\Omega)}}$ *associated to the following inner product*

$$(u, v)_{V(\Omega)} = \int_\Omega \nabla_x u\nabla_x v\mathrm{d}x + \int_\Gamma \mathrm{Re}(\alpha(x))uv\mathrm{d}\sigma. \tag{2}$$

Then for all $f \in L_2(\Omega)$ *and* $g \in B^{2,2}_\beta(\Gamma_D)$ *(with* $\beta = 1 - \frac{n-d}{2} > 0$*) and* $\omega > 0$ *there exists a unique* u*, such that* $(u - g) \in V(\Omega)$*, the solution of problem*

$$\begin{cases} \triangle u + \omega^2 u = f(x) & x \in \Omega, \\ u = g(x) \quad on\ \Gamma_D, & \dfrac{\partial u}{\partial n} = 0 \quad on\ \Gamma_N, \quad \dfrac{\partial u}{\partial n} + \alpha(x)u = 0 \quad on\ \Gamma, \end{cases} \tag{3}$$

in the following weak sense: for all $v \in V(\Omega)$

$$\int_\Omega \nabla u \cdot \nabla\bar{v}\mathrm{d}x - \omega^2 \int_\Omega u\bar{v}\mathrm{d}x + \int_\Gamma \alpha u\bar{v}\mathrm{d}m_d = -\int_\Omega f\bar{v}\mathrm{d}x. \tag{4}$$

The weak solution u continuously depends on the data: there exists $C > 0$, not depending on f, g and the values of α, such that

$$\|u\|_{H^1(\Omega)} \leq C \left(\|f\|_{L^2(\Omega)} + \|g\|_{B^{2,2}_{\beta}(\Gamma_D)} \right). \tag{5}$$

Proof. Let us focus on the proof of the second point in Theorem 2, *i.e.* on the well-posedness of the Helmholtz system (3). We consider the space $V(\Omega)$, defined in Point 1 of the Theorem, with the norm, associated to (2) with $u_2 = v_2 = 0$. Thanks to the continuity of the trace operator $\mathrm{Tr} : H^1(\Omega) \to L_2(\Gamma_D)$, the space $V(\Omega)$ is a Hilbert space with the inner product of $H^1(\Omega)$. As Γ is a part of a compact boundary $\partial\Omega$, the norms $\|\cdot\|_{H^1(\Omega)}$ and $\|\cdot\|_{V(\Omega)}$ are equivalent on $H^1(\Omega)$ (by (3) from Ref. [2]). Thus, the space $V(\Omega)$ is also a Hilbert space with the inner product, defined by (2). First, we consider the boundary value problem for the Laplacian ($\omega = 0$). We define a sesquilinear form $a(\cdot,\cdot)$ and an anti-linear form on $V(\Omega)$ respectively by

$$a(u,v) = \int_\Omega \nabla u \cdot \nabla \bar{v} \mathrm{d}x + \int_\Gamma \alpha u \bar{v} \mathrm{d}m_d, \quad l(v) = \int_\Omega f \bar{v} \mathrm{d}x.$$

We are looking for the weak solution $u \in V(\Omega)$ of the following variational problem

$$\forall v \in V(\Omega), \quad a(u,v) = l(v).$$

We apply the complex version of the Lax-Milgram theorem on $V(\Omega)$. The coercivity and the continuity of the form $a(\cdot,\cdot)$ are immediate. Thanks to the boundness of Ω, the Poincaré inequality holds on $V(\Omega)$ and allows us to show the continuity of l:

$$|l(v)| \leq \|f\|_{L^2(\Omega)} \|v\|_{L^2(\Omega)} \leq C(\Omega) \|f\|_{L^2(\Omega)} \|v\|_{V(\Omega)}.$$

Using now Theorem 1, which ensures that the extension operator $H^1(\Omega)$ into $H^1(\mathbb{R}^n)$ is continuous and that the embedding $H^1(\Omega)$ to $L^2(\Omega)$ is still compact, we conclude that, as in the usual case of a regular boundary, the operator $-\Delta$ with the boundary conditions imposed in the weak sense (see Eq. (4)) has a discrete spectrum and a compact resolvent

$$\forall v \in V(\Omega) \quad (u,v)_{V(\Omega)} + i \int_\Gamma \mathrm{Im}(\alpha) u \overline{v} \mathrm{d}m_d = \lambda \int_\Omega u \overline{v} \mathrm{d}x. \tag{6}$$

Now let us prove that a real number ω^2 is not an eigenvalue of $-\Delta$. Suppose the converse: there exists an eigenfunction $u \in V(\Omega)$, such that (6) holds for $\lambda = \omega^2 \in \mathbb{R}^+$. Therefore, it also holds for $v = u$ and implies that $\int_\Gamma \mathrm{Im}(\alpha)|u|^2 \mathrm{d}m_d = 0$. As $\mathrm{Im}(\alpha) < 0$, it implies, that $\mathrm{Tr}u|_\Gamma = 0$ and consequently, by the week Robin condition on Γ, $\frac{\partial u}{\partial n}|_\Gamma = 0$ in the distributional sense

$$\forall v \in H^1(\Omega) \quad \int_\Omega \Delta u \overline{v} \mathrm{d}x = -\int_\Omega \nabla u \cdot \nabla \overline{v} \mathrm{d}x.$$

Then $u \equiv 0$, what follows from the uniqueness of the solution to the Cauchy problem for $\nabla + \omega^2$ with the Cauchy data on Γ (see [10] Theorem 1.1 with the proof using the connected property of Ω on p. 11 and Theorem 1.2 on p. 12, which can be directly updated on the case of a domain Ω with a d-set boundary satisfying the conditions of Theorem 1). Consequently, the Helmholtz system (3) is well-posed for all $\omega \in \mathbb{R}$ in the weak sense of (4). Thus, as a corollary of the Fredholm theorem, we also have estimation (5). □

We finish this section by a direct corollary of Theorem 2.2 [23] and Theorem 2

Theorem 3 *Let Ω be a bounded domain in $\mathbb{R}^n$ satisfying the conditions of Theorem 1 with a closed d-set boundary $\partial\Omega = \Gamma_D \cup \Gamma_N \cup \Gamma$ ($n-2 < d < n$). By m_d is denoted the d–dimensional Hausdorff measure on $\partial\Omega$ (see Definition 1). Let in addition $\mathrm{Re}(\alpha(x)) > 0$, $\mathrm{Im}(\alpha(x)) < 0$ be continuous functions on Γ. Then the following problem*

$$\begin{cases} \triangle u + \omega^2 u = f(x) \quad x \in \Omega, \\ u = 0 \quad on\ \Gamma_D, \quad \dfrac{\partial u}{\partial n} = 0 \quad on\ \Gamma_N, \quad \dfrac{\partial u}{\partial n} + \alpha(x)\mathrm{Tr}\, u = \mathrm{Tr}\, h(x) \quad on\ \Gamma, \end{cases} \tag{7}$$

has a unique weak solution $u \in V(\Omega)$ for all $f \in L^2(\Omega)$ and $h \in V(\Omega)$ in the following sense: for all $v \in V(\Omega)$

$$\int_\Omega \nabla u \cdot \nabla \bar{v} \mathrm{d}x - \omega^2 \int_\Omega u\bar{v}\mathrm{d}x + \int_\Gamma \alpha \mathrm{Tr}\, u \mathrm{Tr}\, \bar{v} \mathrm{d}m_d = -\int_\Omega f\bar{v}\mathrm{d}x + \int_\Gamma \mathrm{Tr}\, h \mathrm{Tr}\, \bar{v}\mathrm{d}m_d. \tag{8}$$

The weak solution u continuously depends on the data: there exists $C > 0$, independent of f, h and the values of α, such that

$$\|u\|_{V(\Omega)} \le C\left(\|f\|_{L^2(\Omega)} + \|h\|_{V(\Omega)}\right). \tag{9}$$

In particular, for all fixed $\omega > 0$ the operator

$$B : L^2(\Omega) \times L^2(\Gamma) \to V(\Omega), \ \textit{defined by}\ B(f, \mathrm{Tr}\, h) = u$$

with u, the weak solution of problem (7), is compact.

Proof. The continuity of B is evident and equivalent to estimate (9). Let us prove that for any fixed $\omega > 0$ B is also compact (see also Ref. [2] for the real Robin boundary condition). Indeed, let $(f_j, \mathrm{Tr}\, h_j) \rightharpoonup (f, h)$ in $L_2(\Omega) \times L_2(\Gamma)$. Taking for all $j \in \mathbb{N}$ $u_j = B(f_j, \mathrm{Tr}\, h_j)$ and $u = B(f, \mathrm{Tr}\, h)$, by the continuity of B it follows that $u_j \overset{V(\Omega)}{\rightharpoonup} u$. Knowing in addition that $\mathrm{Tr} : V(\Omega) \to L_2(\Gamma)$ and the inclusion of $H^1(\Omega)$ in $L_2(\Omega)$ are compact (see Ref. [2]), with the choice of $v = u_j$ in the variational formulation (8) we find

$$\|u_j\|^2_{V(\Omega)} = \omega^2 \|u_j\|^2_{L^2(\Omega)} - i\int_\Gamma \mathrm{Im}\,\alpha |\,\mathrm{Tr}\, u_j|^2 \mathrm{d}m_d - \int_\Omega f_j \overline{u}_j \mathrm{d}x + \int_\Gamma \mathrm{Tr}\, h_j \overline{\mathrm{Tr}\, u_j} \mathrm{d}m_d, \tag{10}$$

and hence,

$$\begin{aligned} \lim_{j\to+\infty} \|u_j\|^2_{V(\Omega)} =& \omega^2 \|u\|^2_{L^2(\Omega)} - i\int_\Gamma \mathrm{Im}\,\alpha |\,\mathrm{Tr}\, u|^2 \mathrm{d}m_d - \int_\Omega f\overline{u}\mathrm{d}x + \int_\Gamma \mathrm{Tr}\, h \overline{\mathrm{Tr}\, u} \mathrm{d}m_d \\ &= \|u\|^2_{V(\Omega)}. \end{aligned}$$

Having both $u_j \rightharpoonup u$ in $V(\Omega)$ and $\|u_j\|_{V(\Omega)} \to \|u\|_{V(\Omega)}$ implies that $u_j \to u$ in $V(\Omega)$ and hence B is compact. Since the norm $\|u\|^2_{V(\Omega)}$ on $V(\Omega)$ is equivalent to the norm

$$\|u\|^2_J = A\|u\|^2_{L_2(\Omega)} + B\|\nabla u\|^2_{L_2(\Omega)} + C\|u\|^2_{L_2(\Gamma)},$$

the operator B is also compact corresponding to this norm. $\square$

3 Shape design problem for a range of frequencies

From Section 3 of Part I [23] Theorem 3.2, we know that for all fixed $\omega > 0$, if $\partial\Omega_0$ is Lipschitz, then there exits an optimal shape $\Omega^{opt} \in U_{ad}(\Omega_0)$, minimizing the acoustic energy

$$J(\Omega)(\omega) = A(\omega)\int_\Omega |u|^2 \mathrm{d}x + B(\omega)\int_\Omega |\nabla u|^2 \mathrm{d}x + C(\omega)\int_\Gamma |u|^2 d\sigma \tag{11}$$

on all admissible shapes of Γ, keeping constant the volume of the initial domain Ω_0. We recall the definition of the admissible class of domains [23] included in a fixed Lipschitz domain D and containing Γ in a fixed open set G in D

$$U_{ad}(\Omega_0) = \{\Omega \in \mathcal{C}(\Omega_0)|\ d(\Omega,\Omega_0) \leq \frac{1}{8},\ \Gamma_D \cup \Gamma_N \subset \partial\Omega,\ \int_\Omega \mathrm{d}x = \mathrm{Vol}(\Omega_0)\}, \tag{12}$$

where $\mathcal{C}(\Omega_0) = \{\Omega \subset D|\ \Gamma \subset \overline{G}$ and $\exists\theta \in W^{1,\infty}(\mathbb{R}^2,\mathbb{R}^2),\ \|\theta\|_{W^{1,\infty}(\mathbb{R}^2,\mathbb{R}^2)} < 1$ such that $\Omega = (Id+\theta)\Omega_0\}$. In what follows we also suppose that A, B and C are C^1 positive functions of ω. In the definition of $U_{ad}(\Omega_0)$ we take $d(\Omega,\Omega_0) \leq \frac{1}{8}$ according to Lemma 2.4 in Ref. [25] in the case $n = 2$ and $k = 1$. Here, by [1, 25], d is the quasi-distance $d(\Omega,\Omega_0)$ on $\mathcal{C}(\Omega_0)$. If $d_H(\Omega_0,\Omega)$ is the Hausdorff distance between Ω_0 and Ω, we know [25] that $d_H(\Omega_0,\Omega) \leq d(\Omega_0,\Omega)$.

Let us notice that a bounded domain with a Lipschitz boundary is a particular case of the (ε,δ)-domains and hence the optimal shape domain is also an (ε,δ)-domain. For practical reasons, it is more realistic to find "the simplest" optimal shape, thus the general fractal or (ε,δ)-domains case is not really of interest. In addition, in most practical situations we need to find "the simplest" optimal shape not only for a fixed frequency, but for a large frequency interval $[\omega_0,\omega_1]$, such that walls with such a shape could actually be manufactured. Hence, in the aim to find the simplest shape, efficient for the energy dissipation in a range of frequencies, we introduce the definition of an ε-optimal shape:

Definition 4 (ε-optimal domain) *The domain $\Omega^* \in U_{ad}(\Omega_0)$ is called an ε-optimal domain for the range of frequencies $[\omega_0,\omega_1]$, if for all $\omega \in [\omega_0,\omega_1]$ it holds*

$$|\min_{\Omega\in U_{ad}(\Omega_0)} J(\Omega)(\omega) - J(\Omega^*)(\omega)| < \varepsilon,$$

where by $J(\Omega^*)(\omega)$ is denoted the value of the functional J, calculated for the domain Ω^* at the frequency ω.

Remark 2 *To validate the notion of ε-optimal domain, let us verify that for a fixed $\varepsilon > 0$, if Ω^* is optimal for ω^*, there exists an interval $[\omega_0,\omega_1]$, such that $\omega^* \in [\omega_0,\omega_1]$, for which Ω^* is ε-optimal. Actually, we notice that*

- *u depends continuously on ω and Ω;*
- *for a fixed frequency, J is continuous as a function of Ω;*

- *as the functional* J *is continuous with respect to* $\omega \in \mathbb{R}^+$, *it is equicontinuous on all compacts in* $\mathbb{R}^+$:

$$\forall \eta > 0 \quad \exists \delta_1(\eta) > 0 : |\omega^* - \omega| < \delta_1 \Rightarrow |J(\Omega^*)(\omega^*) - J(\Omega^*)(\omega)| < \eta;$$

- $J_{\min}(\omega) := \min_{\Omega \in U_{ad}} J(\Omega)(\omega)$ *is a uniquely defined continuous function of* ω:

$$\forall \hat{\eta} > 0 \quad \exists \delta_2(\hat{\eta}) > 0 : |\omega^* - \omega| < \delta_2 \Rightarrow |\min_{\Omega \subset U_{ad}(\Omega_0)} J(\Omega)(w) - J(\Omega^*)(\omega^*)| < \hat{\eta}.$$

Therefore, for a fixed $\varepsilon > 0$, *we choose* $\eta = \hat{\eta} = \frac{\varepsilon}{2}$, *there exists* $\delta(\varepsilon) > 0$ *(actually,* $\delta = \min(\delta_1, \delta_2)$*), such that, if* $|\omega^* - \omega| < \delta$, *we have*

$$|\min_{\Omega \subset U_{ad}(\Omega_0)} J(\Omega)(\omega) - J(\Omega^*)(\omega)| \\ \leq |\min_{\Omega \subset U_{ad}(\Omega_0)} J(\Omega)(\omega) - J(\Omega^*)(\omega^*)| + |J(\Omega^*)(\omega^*) - J(\Omega^*)(\omega)| \leq \varepsilon.$$

Since wall performances depend on the sizes of its components compared to the wavelengths of the source, we firstly introduce, according to the physical meaning and numerical results from Section 4.1, the following definition of a "much smaller" wavelength and of "a much higher" frequency:

Definition 5 *Let* $\omega_1 > 0$ *be a fixed frequency. A frequency* ω_2 *is called a much higher frequency for* ω_1, $\omega_2 \gg \omega_1$, *if* $\omega_2 \geq 2\omega_1$. *Consequently, for the wavelengths:* $\lambda_2 \ll \lambda_1$ *(*λ_2 *is much smaller then* λ_1*), if* $\lambda_2 \leq \frac{\lambda_1}{2}$. *Conversely, the wavelength* λ *is called comparable to* λ_0, *if* $\lambda \in]\frac{\lambda_0}{2}, 2\lambda_0[$.

Next, let us define the notion of the characteristic geometry size of a domain Ω (or Γ, since only the boundary Γ with the Robin boundary condition can change its shape). If Γ starts at a point $x_B \in \partial\Omega$ and ends at a point $x_E \in \partial\Omega$, we consider γ_0, which connects the points x_B and x_E by a straight line. For $x = (x^1, x^2) \in \mathbb{R}^2$, we suppose that the first coordinate axis x^1 follows γ_0 and the second coordinate axis x^2 follows its normal direction. Since, the boundary Γ belongs to a fixed area $\overline{G}$, chosen in the beginning, the largest geometrical size of Γ parallel to x^2 depends on the chosen G. Thus, we does not consider the geometries with parts having a length along the axis x^1 much smaller the length along x^2, and we especially interested in the shape sizes projected on x^1.

Definition 6 (Shape lengths of Ω**)** *Let the boundary* Γ *be a* C^1 *boundary of* Ω *starting from the point* $x_B = (x_B^1, 0)$ *and ending in* $x_E = (x_E^1, 0)$ *and* γ_0 *be the straight line (*$x_2 = 0$*) connecting these two points (see Fig. 1 for an example). We suppose that* Γ *can be locally defined by the graph of a* C^1 *function (each time denoted by* f, $f(x) = 0$ *for* $x \in \Gamma$*). By* $x_i = (x_i^1, 0)$ *(*$i = 1, \ldots, N$*) are denoted the intersection points of* Γ *with* γ_0, *ordered by the first coordinate from left to right*

$$x_0^1 = x_B^1 < x_1^1 < x_2^1 < \ldots < x_N^1 < x_E^1 = x_{N+1}^1, \tag{13}$$

for which in any neighborhood V *of* x_i *there exists* $x \in \Gamma$ *such that* $\frac{\partial}{\partial n} f(x) = \partial_{x_2} f \neq 0$. *Here* $n = (0, 1)$ *is the unit normal vector to* γ_0. *These points define the deviation parts*

of Γ *compared to the straight line* γ_0 *(see the filled regions on Fig. 1 and Fig. 2). Thus, we define the "horizontal" lengths*

$$h_i = |x_i^1 - x_{i-1}^1| \quad for \quad i = 1, \dots, N+1.$$

Let, for $x \in \gamma_0$, $m(x)$ *be the number of intersections with* Γ *of the vertical line, passing by the point* x, *denoted by* $L(x)$.

If on a part of Γ, *limited by two lines* $L(x_{i-1})$ *and* $L(x_i)$, *the relation* $f(x) = 0$ *defines a bijection between* x^1 *and* x^2, *i.e. for all* $x \in \gamma_0$ *with* $x^1 \in]x_{i-1}^1, x_i^1[$, $m(x) = 1$, *we write* $x^2 = g(x^1)$ *and we define on* $]x_{i-1}^1, x_i^1[$ *(see Fig. 2)*

$$g_{up}(x^1) = \max(0, g(x^1)) \quad and \quad g_{low}(x^1) = \min(0, g(x^1)).$$

Thus, we find the "vertical" lengths for each of such geometrical parts, by setting

$$v_i = \sup_{x^1 \in [x_{i-1}^1, x_i^1]} |g_{up}(x^1) - g_{low}(x^1)| = \sup_{x^1 \in [x_{i-1}^1, x_i^1]} |g(x^1)|,$$

and form the couples (h_i, v_i).

We now consider maximum intervals $[x_{j,B}^*, x_{j,E}^*] \subset]x_B^1, x_E^1[$ *on which* $m(x) > 1$, *(i.e. if* $x = x_{j,B}^* - \varepsilon$ *or* $x = x_{j,E}^* + \varepsilon$ *for all sufficiently small* $\varepsilon > 0$, *then* $m(x) = 1$*) and define on* $[x_{j,B}^*, x_{j,E}^*]$ *functions* $g_B(x^1)$ *and* $g_E(x_1)$ *taking respectively the value of the first and the last intersection of* $L(x^1)$ *with* Γ *following the normal direction to* γ_0 $n = (0, 1)$. *Then we define on* $[x_{j,B}^*, x_{j,E}^*]$

$$f_{up}(x^1) = \max(0, g_E(x^1)) \quad and \quad f_{low}(x^1) = \min(0, g_B(x^1)).$$

Therefore, we set

$$h_j^* = |x_{j,E}^* - x_{j,B}^*|, \quad v_j^* = \sup_{x^1 \in [x_{j,B}^*, x_{j,E}^*]} |f_{up}(x^1) - f_{low}(x^1)|$$

and we fix, as previous, the couples (h_j^*, v_j^*).

Going in smaller geometrical details, on each bijection interval $[x_i^1, x_{i-1}^1]$ *with* $m(x) = 1$ *we consider all points* $\tilde{x}_l^1$ *for* $l = 1, \dots, K$ *for which*

$$\partial_{x^1} g(\tilde{x}_l^1) = 0 \quad and \quad \tilde{x}_j^1 \neq \tilde{x}_{j+1}^1.$$

Let us set $\tilde{x}_0 = x_{i-1}$ *and* $\tilde{x}_{K+1} = x_i$. *If* $K \geq 3$ *is an odd number (i.e. the derivative changes its sign more than twice between* $L(x_{i-1})$ *and* $L(x_i)$*), then we set (as* K *is odd, then* $K + 1$ *is even)*

$$\tilde{h}_l = |\tilde{x}_{2l}^1 - \tilde{x}_{2(l-1)}^1|, \ \tilde{v}_l = \sup_{x^1 \in [\tilde{x}_{2(l-1)}^1, \tilde{x}_{2l}^1]} |g(x^1)| \ for \ l = 1, \dots, \frac{K+1}{2}.$$

To avoid difficult notations, the obtained sequence

$$(h_i, v_i)_{i=1\dots N} \cup (h_j^*, v_j^*)_{j=1\dots N^*} \cup (\tilde{h}_l, \tilde{v}_l)_{l=1,\dots,\frac{K+1}{2}}$$

is still denoted by $(h_i, v_i)_{i=1\ldots N}$.

If there exists $x \in \gamma_0$ *, such that* $x^1 \in]x^1_{i^*}, x^1_{i^*+1}[$ *for a fixed* i^* *in the subdivision (13) and* $m(x) > 1$ *, then the corresponding part of* Γ *, given by* f *, does not define anymore a bijection* g *between* x^1 *and* x^2 *for* $x^1 \in]L(x_{i^*}), L(x_{i^*+1})[$ *. Let us consider the union of the joint intervals* $]x^1_{i^*}, x^1_{i^*+k}[$ *(*$k \geq 1$ *) on which the graph of* f *is not bijective. Then, going from the left to the right on* Γ *inside of the area delimited by* $L(x_{i^*})$ *and* $L(x_{i^*+k})$ *, we find points* $y_j \in \Gamma$ *(*$j \in \mathbb{N}$ *), such that*

$$\partial_{x^2} f(y_j) = 0 \quad \textit{and} \quad y^1_j \neq y^1_{j+1}.$$

Hence, we define the horizontal lengths $h_{N+j} = |y^1_{j+1} - y^1_j|$*. To define the vertical lengths we say that a curve in the found bijection area is the lower geometrical part* f_l *, if the number of intersections of* $L(x)$ *with it is odd (*$m(x)$ *is odd) and is the upper part* f_u *, if the number of intersections with it is even (see Fig. 2). Therefore, we define* h_{N+j} *as* $\|f_u - f_l\|_{C(I)}$ *in the bijective compact segment* I *, constructed using the points* x_i *and the projections on* γ_0 *of points* y_j *.*

For each bijective interval inside of $]x^1_{i^*}, x^1_{i^*+1}[$ *, actually between all couples of points* (y_{j-1}, y_j) *, we also find, as for the bijective case, all points* $\tilde{y}_k$ *for* $k = 1, \ldots, K$ *, for which* $\partial_{x^2} f(\tilde{x}_k) = 0$ *, and, in the case of* $K \geq 3$ *, we add* $\tilde{h}_k = |\tilde{y}^1_{2k} - \tilde{y}^1_{2(k-1)}|$ *and* $\tilde{v}_k = \|f_u - f_l\|_{C([\tilde{x}^1_{2(k-1)}, \tilde{x}^1_{2k}])}$ *for* $k = 1, \ldots, \frac{K+1}{2}$ *to the sequence* $(h_i, v_i)_{i=1\ldots N}$ *.*

Repeating the above procedure for all intervals (or more generally, for all unions of joint intervals) on γ_0 *, where at least in one point* $m(x) > 1$ *, we construct the sequence* $(h_i, v_i)_{i\in\mathbb{N}}$ *, finite or not. Now, for each* i *we compare* h_i *and* v_i *:*

1. *if* $v_i \ll h_i$ *, then* $d_i := h_i$ *(the fragment is a quasi-plane),*
2. *if* v_i *and* h_i *are comparable, then* $d_i := \frac{h_i + v_i}{2}$ *.*

The case $h_i \ll v_i$ *is forbidden by the assumption and by the choice of the open set* G *. The lengths* $(d_i)_{i\in\mathbb{N}}$ *are characteristic lengths of each element of* Γ *compared to* γ_0 *and are called shape's length of* Ω *.*

Definition 7 (Characteristic geometric size of Ω) *Let* $(d_i)_{i\in\mathbb{N}}$ *be the sequence of shape lengths of* Ω *. Independently of the fact is it finite or not, there exists the length* $d = \max_i d_i$ *, which is called the largest geometric size of* Ω *. If the length of* Γ *is finite, then the number of its shape lengths* N *is finite too, and there exists the minimal geometric size* $d_{\min} = \min\limits_{i=1,\ldots,N} d_i$ *. Hence, let* $(d_i)_{i\in\mathbb{N}}$ *be ordered decreasing by*

$$d = d_0 \geq d_1 \geq d_2 \geq \ldots, \quad d_i \to 0 \textit{ if } i \to +\infty \textit{ or } d_N = d_{\min} \textit{ if } N < \infty.$$

The sequence (d_i) *defines the distribution of geometrical sizes of* Γ *. Let* $\mathrm{Vol}(\gamma_0)$ *be the length of* γ_0 *:* $\mathrm{Vol}(\gamma_0) = |x_E - x_B|_{\mathbb{R}^2}$ *. A positive number* $\ell_k(\Omega)$ *(*$k \in \mathbb{N}$*) is a characteristic geometric size of* Ω *number* k *if there exists* $K(k) \geq 2^k \left[\frac{\mathrm{Vol}(\gamma_0)}{2d}\right]$ *shape lengths of* Ω

$$d_{i_m} \in \left]\frac{d}{2^{k+1}}, \frac{d}{2^{k-1}}\right[\cap [d_{\min}, d] \quad (m = 0, \ldots, K(k)) \textit{ such that } \ell_k(\Omega) = \frac{1}{K(k)} \sum_{m=1}^{K(k)} d_{i_m}.$$

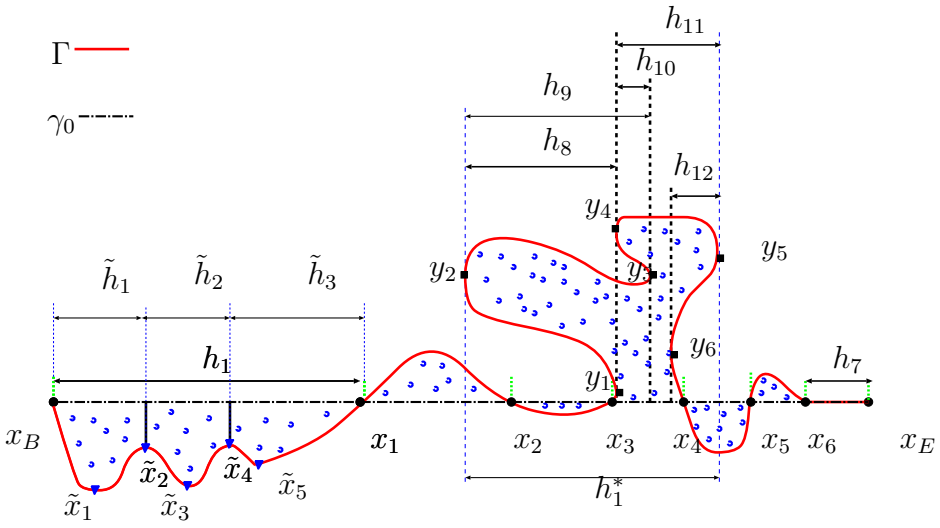

Figure 1: Example of the definition of horizontal shape lengths of Γ by the construction introduced in Definition 6. Here we have 6 intersections of Γ with γ_0 and 6 additional points y_i in the region $]x_1^1, x_5^1[$, where there are points $x \in \gamma_0$ for which $m(x) > 1$. The segment $[x_B^1, x_1^1]$ contains the projections of 5 points $\tilde{x}_i$, in which the tangential derivative of f parallel to γ_0 is equal to zero, $\partial_{x^1} f(x) = 0$. The maximum interval $[y_2^1, y_5^1]$, where $m(x) > 1$, gives the length h_1^*. Therefore, the sequence of the horizontal shape lengths is given by h_i for $i = 1, \ldots, 11$, h_1^* and $\tilde{h}_l$ for $l = 1, 2, 3$. The intervals, on which Γ can be described by a bijection for $x^1 \in [y_2^1, y_5^1]$, are $[x_2^1, x_3^1]$, $[x_3^1, y_1^1]$, $[y_2^1, y_1^1]$, $[y_1^1, y_3^1]$, $[y_4^1, y_3^1]$, $[y_3^1, y_6^1]$, $[y_6^1, y_5^1]$, $[y_6^1, x_4^1]$.

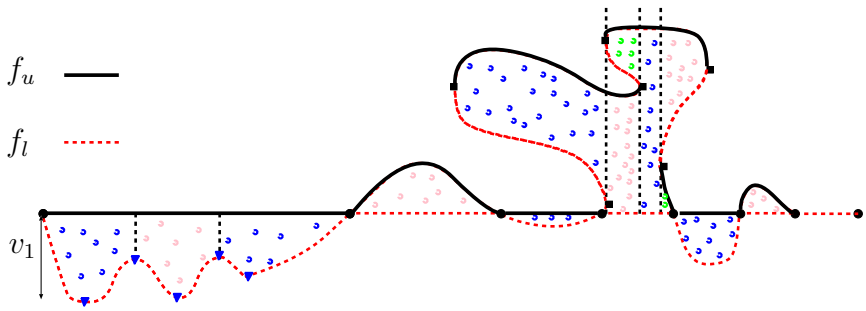

Figure 2: The choice of f_u and f_l for each interval, where Γ given on Fig. 1 is defined by a bijection.

If $k = 0$, $\ell_0(\Omega)$, denoted in what follows by $\ell(\Omega)$, is the largest characteristic geometry size of Ω. If $k \in \mathbb{N}$ is such that $\frac{d}{2^{k+1}} \leq d_{\min} < \frac{d}{2^{k-1}}$, then the corresponding $\ell_k(\Omega)$, denoted in what follows by $\ell_{\min}(\Omega)$, is the smallest characteristic geometric size of Ω.

Let us also formulate the physical principle:

Assumption 1 (Physical principle) *Let* $\omega_0 = \frac{2\pi}{\lambda_0}$ *and* Ω_{λ_0} *be a domain with the unique characteristic geometric size* $\ell(\Omega_{\lambda_0}) = \ell_{min}(\Omega_{\lambda_0}) = \frac{\lambda_0}{2}$.

- *A wave with a wavelength* λ_0 *does not fit into a shape of characteristic scale much smaller than* λ_0 *: there exists* $\lambda_{\min} > 0$ *(*$\lambda_{\min} \ll \lambda_0$ *) such that*

$$\forall \lambda \in]0, \lambda_{\min}] \quad J(\Omega_\lambda)(\omega_0) = J(\Omega_{\lambda_{\min}})(\omega_0) = J(\Omega_{\lambda_0})(\omega_0),$$

  where by Ω_λ *for* $\lambda < \lambda_0$ *is denoted a domain constructed from* Ω_{λ_0} *by adding to* Γ_{λ_0} *smaller scales of the characteristic size* $\frac{\lambda}{2}$.

- *If the wave interaction with the dissipative media increases, then the energy of the wave decreases. More precisely, let* Ω *be a domain with* $\ell(\Omega) = \ell(\Omega_{\lambda_0})$, $\ell_{min}(\Omega) \ll \ell_{min}(\Omega_{\lambda_0})$ *and* $d_H(\Omega, \Omega_{\lambda_0}) \leq \ell_{min}(\Omega)$ *. Then the domain* Ω *has two different scales:* $\ell(\Omega)$ *and* $\ell_{min}(\Omega)$ *. Actually, we suppose that the boundary* Γ *of the domain* Ω *is obtained by adding to* Γ_{λ_0} *smaller scales. Adding a scale to the boundary of* Ω_{λ_0} *, we increase the wave interaction with the dissipative part of the boundary. Therefore, the energy* $J(\Omega)(\omega_0)$ *can only decrease, as compared to* $J(\Omega_{\lambda_0})(\omega_0)$ *, or stay equal (in the case of no fitting of the wave inside the smallest parts of the boundary). Thus, if* $\Omega^o_{\lambda_0}$ *is an optimal domain for the frequency* ω_0 *, then we have*

$$J(\Omega^o_{\lambda_0})(\omega_0) \leq J(\Omega)(\omega_0) \leq J(\Omega_{\lambda_0})(\omega_0).$$

We also use the following hypothesis, coming from the empirical physics and confirmed by the numerical results in Section 4.1:

Assumption 2 *Let* Ω^* *be an optimal domain for* $\omega^* > 0$ *with* n $(n \in \mathbb{N})$ *characteristic geometric scales* $(\ell_j(\Omega^*))_{j=0,\ldots,n-1}$ *. Then there exists* j_0 $(0 \leq j_0 \leq n-1)$ *, such that* $\ell_{j_0}(\Omega^*) = \frac{\lambda^*}{2}$.

In the framework of ε -optimal shapes, the physical principle with Definition 5 directly ensures

Proposition 1 *1. Let* Ω^* *be an optimal domain for* $\omega^* > 0$ *with* n $(n \in \mathbb{N})$ *characteristic geometric scales, such that* $\ell_{j_0}(\Omega^*) = \frac{\lambda^*}{2}$ *with* $0 \leq j_0 \leq n-1$ *, as in Assumption 2. Then any* $\Omega \in U_{ad}(\Omega_0)$ *with the same characteristic geometric scales as* Ω^* *up to number* j_0 *:*

$$\forall\, j = 0, \ldots, j_0 \quad \ell_j(\Omega) = \ell_j(\Omega^*),$$

and $d_H(\Omega, \Omega^*) < \frac{\lambda^*}{4}$ *, is also optimal on* ω^* *:*

$$J(\Omega)(\omega^*) = J_{\min}(\omega^*) = J(\Omega^*)(\omega^*).$$

2. Let $\varepsilon > 0$ *be a fixed real number and* $\Omega \in U_{ad}(\Omega_0)$ *(see Eq. (12)) for the definition of* $U_{ad}(\Omega_0)$ *) be an* ε *-optimal domain on a range of frequencies* $[\omega_0, \omega_1]$ *with the smallest characteristic geometric size:*

$$\ell_{\min}(\Omega) = \frac{\lambda}{2} \quad \text{for some } \lambda \in [\lambda_1, \lambda_0].$$

If $\Omega^o \in U_{ad}(\Omega_0)$ *is a domain, such that*

$$\exists j \in \mathbb{N}: \quad \ell_j(\Omega^o) = \ell_{\min}(\Omega) \quad \text{and } d_H(\Omega^o, \Omega) \leq \frac{\lambda}{4},$$

then Ω^o *is also* ε*-optimal on* $[\omega_0, \omega_1]$ *(with the same* ε*).*

Proof. Let us prove the first point. Without loss of generality, let us suppose Ω^* is such that $j_0 = n-1$, *i.e.* $\ell_{\min}(\Omega^*) = \frac{\lambda^*}{2}$. Thus, if Ω has additional characteristic geometric sizes $\ell_j \ll \frac{\lambda^*}{2}$ $(j \geq n)$ with $d_H(\Omega, \Omega^*) < \frac{\lambda^*}{4}$, then by Assumption 1, the greater interaction of the wave with the dissipative boundary implies the non increasing of the energy $J(\Omega)(\omega^*) \leq J(\Omega^*)(\omega^*)$. But, since Ω^* is optimal on ω^*, we also have $J(\Omega^*)(\omega^*) = J_{\min}(\omega^*) \leq J(\Omega)(\omega^*)$. Consequently, $J(\Omega)(\omega^*) = J_{\min}(\omega^*)$, which ensures that Ω is optimal on ω^*. Therefore, to be optimal on a fixed frequency ω^*, it is sufficient to be optimal for the geometric sizes with $\ell = \frac{\lambda^*}{2}$, all sizes much smaller than $\frac{\lambda^*}{2}$ (in the sense of $d_H(\Omega^*, \Omega) \leq \frac{\lambda^*}{4}$), do not change the optimal property at one frequency point.

Let us prove the second point. Since Ω is ε-optimal on $[\omega_0, \omega_1]$, we have: for all $\omega \in [\omega_0, \omega_1]$ $|J(\Omega)(\omega) - J_{\min}(\omega)| < \varepsilon$. If we keep this scale and add characteristic scales much smaller than $\lambda/2$, such that $d_H(\Omega^o, \Omega) \leq \frac{\lambda}{4}$, then it holds $J_{\min}(\omega) \leq J(\Omega^o)(\omega) \leq J(\Omega)(\omega)$. From this inequality, we directly have

$$|J(\Omega)(\omega) - J(\Omega^o)(\omega)| \leq |J(\Omega)(\omega) - J_{\min}(\omega)| < \varepsilon,$$

i.e., since the adding of small characteristic scales does not change the properties to be optimal on ω, it also does not change the property to be not farther than ε from the optimal domain. Hence, the properties of ε-optimality still hold for Ω^o with the same ε. □

Remark 3 *Thanks to the first point of Proposition 1, in what follows, for a solution of* $\min_{\Omega \in U_{ad}} J(\Omega)(\omega)$ *we always take* Ω *with* $\ell_{min}(\Omega) = \frac{\lambda}{2}$ *(for* $\lambda = 2\pi/\omega$*) (i.e. we consider the "simplest" such* Ω *in terms of characteristic scales).*

Definition 8 (*n*-times wavelength preserving optimal domain) *Let* Ω_{λ_0} *be a fixed initial domain with at least Lipschitz boundary,* $\lambda_0 = \frac{2\pi}{\omega_0} \leq \frac{1}{2}$ *for a fixed* $\omega_0 \geq 4\pi$ *and* $n \geq 1$, $n \in \mathbb{N}$. *The domain* $\Omega^{opt} \in U_{ad}(\Omega_{\lambda_0})$ *is called an* n*-times wavelength preserving optimal domain based on* Ω_{λ_0} *for the frequency* ω_0*, if there exists*

$$\lambda_n < \ldots < \lambda_k < \ldots < \lambda_1 < \lambda_0, \quad \text{such that } \forall\, k = 1, \ldots, n \quad \lambda_k \leq \frac{\lambda_0}{2^k},$$

and $\Omega^{opt} = \Omega_{\lambda_n}$ *is a solution of the following minimization problem (see Eq. (12)) for the definition of the admissible domains)*

$$J(\Omega_{\lambda_n})(\omega_n) = \inf_{\Omega \subset U_{ad}(\Omega_{\lambda_{n-1}}),\, d_H(\Omega, \Omega_{\lambda_{n-1}}) \leq \frac{\lambda_n}{4}} J(\Omega)(\omega_n),$$

where for $k = 1, \ldots, n-1$ *the domains* Ω_{λ_k} *are solutions of the minimization problems*

$$J(\Omega_{\lambda_k})(\omega_k) = \inf_{\Omega \subset U_{ad}(\Omega_{\lambda_{k-1}}),\, d_H(\Omega, \Omega_{\lambda_{k-1}}) \leq \frac{\lambda_k}{4}} J(\Omega)(\omega_k).$$

Remark 4 *We know that* $d_H(\Omega_{\lambda_0}, \Omega) \leq d(\Omega_{\lambda_0}, \Omega)$. *In Definition 8 we have supposed that the largest wavelength* $\lambda_0 \leq \frac{1}{2}$ *(or the smallest frequency* $\omega_0 \geq 4\pi$*) in the aim to ensure* $d_H(\Omega_{\lambda_0}, \Omega) \leq \frac{\lambda_0}{4} \leq \frac{1}{8}$, *where* $\frac{1}{8}$ *comes from the condition from Lemma 2.4 in Ref. [25]. The additional restriction* $d_H(\Omega_{\lambda_k}, \Omega_{\lambda_{k-1}}) \leq \frac{\lambda_k}{4}$ *keeps the new set of the admissible domains closed by the Hausdorff convergence and, thus, we still have the existence of an optimal shape in this class [14, 25].*

Proposition 2 *Let* Ω^{opt} *be an* n*-times wavelength preserving optimal domain based on a domain* Ω_{λ_0} *with* $\Gamma_{\lambda_0} \in C^3$ *for the frequency* $\omega_0 \geq 4\pi$ *(thus* $2\lambda_0 \leq 1$*). Then* $\Omega^{opt} \in U_{ad}(\Omega_{\lambda_0})$ *with* $d_H(\Omega_{\lambda_0}, \Omega^{opt}) \leq \frac{\lambda_0}{4}$ *and* Ω^{opt} *has at least* n *multiscale characteristic shape lengths*

$$\ell_k(\Omega^{opt}) = \frac{\lambda_k}{2} \leq \frac{\lambda_0}{2^{k+1}} \quad (k = 1, \ldots, n).$$

Moreover,

1. *for* $n \geq 2$, *every* Ω_{λ_k}, $k = 1, \ldots n-1$ *is an* $(n-k)$*-times wavelength preserving optimal domain based on the domain* Ω_{λ_0} *for the frequency* ω_0,
2. *for all* $k = 1, \ldots, n$, Ω_{λ_k} *has the characteristic geometric sizes of* $\Omega_{\lambda_{k-1}}$ *and* $\ell_k = \ell_{min}(\Omega_{\lambda_k}) = \frac{\lambda_k}{2}$,
3. *if* Ω_{λ_0} *is an* ε*-optimal domain on* $[\omega_a, \omega_b]$ *(*$\omega_a > 0$, $\omega_0 \in [\omega_a, \omega_b]$*) with* $\ell_{\min}(\Omega_{\lambda_0}) = \frac{\lambda_0}{2}$ *and* $\omega_b \leq 2\omega_0$, *then for* $n \geq 1$ *all domains* Ω_{λ_k} $(k = 1, \ldots, n)$ *are* ε*-optimal on* $[\omega_a, \omega_b]$ *(with the same* ε*).*

Proof. Firstly, we notice that for all $n \geq 1$

$$d_H(\Omega_{\lambda_0}, \Omega^{opt}) \leq \frac{1}{4}(\lambda_1 + \ldots + \lambda_n) \leq \frac{\lambda_0}{8}\left(1 + \frac{1}{2} + \ldots + \frac{1}{2^{n-1}}\right)$$
$$= \left(2 - \frac{1}{2^{n-1}}\right)\frac{\lambda_0}{8} = \left(1 - \frac{1}{2^n}\right)\frac{\lambda_0}{4} \leq \frac{\lambda_0}{4}.$$

Application of Assumption 1 and Proposition 1 finishes the proof. Actually, point 2 is also a direct corollary of Assumption 2. More precisely, for point 3, we have that for all $k \geq 1$

$$d_H(\Omega_{\lambda_k}, \Omega_{\lambda_{k-1}}) \leq \frac{\lambda_k}{4} \leq \frac{\lambda_0}{4 \cdot 2^k} \leq \frac{\lambda_b}{4},$$

with $\ell_j(\Omega_{\lambda_k}) = \ell_{\min}(\Omega_{\lambda_j})$ $(0 \leq j \leq k)$ by point 2. Thus, if for all $k \geq 1$ $\frac{\lambda_0}{4 \cdot 2^k} \leq \frac{\lambda_b}{4}$ (*i.e.* for $\lambda_b \geq \frac{\lambda_0}{2}$), by Proposition 1, Ω_{λ_k} is ε-optimal on the interval of ε-optimality of $\Omega_{\lambda_{k-1}}$. $\square$

Definition 9 *The interval* $[\omega_0, \omega_1]$ *is called the maximum interval of* ε*-optimality of a domain* Ω, *if for all* $\omega \in]\omega_0, \omega_1[$ Ω *is* ε*-optimal on* ω, *but no more on* ω_0 *nor on* ω_1*:*

$$\forall \omega \in]\omega_0, \omega_1[\quad |J(\Omega)(\omega) - J_{\min}(\omega)| < \varepsilon, \ \textit{but} \ |J(\Omega)(\omega_i) - J_{\min}(\omega_i)| \geq \varepsilon \ (i = 0, 1).$$

Now, we give the following theorem for the existence of an ε-optimal domain for a fixed range of frequency for the problem (7), *i.e.* with $g = 0$ on Γ_D:

Theorem 4 *Let* $[\omega_0, \omega_{\max}[$ *with* $\omega_0 \geq 4\pi$ *and* $\omega_{\max} \leq +\infty$ *be a fixed frequency interval, and* Ω_0 *be a fixed regular domain in* $\mathbb{R}^2$ $(\Gamma \in C^3)$ *with* $\ell(\Omega_0) = \ell_{\min}(\Omega_0) = \frac{\lambda_0}{2}$.

Define $N = \left[\log_2 \frac{\omega_{\max}}{\omega_0}\right]$ *for* $\omega_{\max} < \infty$. *For all* $\omega \in [\omega_0, \infty[$ *consider*

$$J_{min}(\omega) = \inf_{\Omega \in U_{ad}(\Omega_0)} J(\Omega)(\omega),$$

the minimum of the acoustical energy for the Helmholtz problem (7) with f, h *and* α *smooth functions of* ω *(of the class* C^1*), such that for all fixed* $\omega > 0$ *they satisfy the assumptions of Theorem 3 and in the high frequency limit verify for* $\omega \to +\infty$

$$\frac{f}{\omega^2} \to 0 \text{ in } L_2(D), \quad \frac{h}{\omega^2} \rightharpoonup 0 \text{ and } \frac{h}{|\mathrm{Im}\alpha|} \rightharpoonup 0 \text{ in } V(D), \ \mathrm{Re}\alpha \to c_r \geq 0, \ |\mathrm{Im}\alpha| \to c_i, \quad (14)$$

where c_i *is either a strictly positive constant or* $+\infty$.

Then $J_{min}(\omega) \to 0$ *for* $\omega \to +\infty$ *and there exists* $\delta_0 \geq 0$, *depending on* ω_0, *such that for all* $\varepsilon > \delta_0$ *there exists a domain* $\hat{\Omega}_0 \in U_{ad}(\Omega_0)$ *with* $\frac{\lambda_0}{4} \leq \ell_{\min}(\hat{\Omega}_0) \leq \ell(\Omega_0)$, *which is* ε*-optimal on a maximal interval* $[\omega_0, \omega_1]$ *with* $\omega_1 \geq 2\omega_0$ *(see Definition 9).*

Moreover, there exists $\varepsilon_0 \geq \delta_0$, *depending on* ω_0 *and* $\omega_{\max}$, *such that for all* $\varepsilon > \varepsilon_0$ *there exists an* ε*-optimal domain* Ω^* *on* $[\omega_0, \omega_{\max}[$ *such that* $d_H(\hat{\Omega}_0, \Omega^*) \leq \frac{\lambda_0}{4}$ *and*

1. *for* $\omega_{\max} < \infty$, $\Omega^* \in U_{ad}(\hat{\Omega}_0)$ *with at least* N *characteristic scales* $\ell_k(\Omega^*) \leq \frac{\lambda_0}{2^{k+1}}$ *for* $k = 1, \ldots, N-1$, *where* $\ell_N(\Omega^*) = \ell_{min}(\Omega^*)$;

2. *for* $\omega_{\max} = \infty$, Ω^* *is a fractal domain (an* (ε, ∞)*-domain), obtained as a limit for* $N \to +\infty$ *of the finite case, with* $\ell_k(\Omega^*) \leq \frac{\lambda_0}{2^{k+1}}$ *for* $k \in \mathbb{N}^*$.

Remark 5 *From the theory of the transparent or absorbing boundary conditions, it is known that the increasing of* $|\mathrm{Im}\alpha|$ *corresponds to the increasing of the wave absorption by the boundary* Γ, *while the coefficient* $\mathrm{Re}\alpha$ *corresponds to the reflection by* Γ. *Intuitively, if* $h = 0$, *the condition* $\frac{\partial u}{\partial |x|} + (\mathrm{Re}\alpha - i|\mathrm{Im}\alpha|)u = 0$ *is satisfied by the wave* $e^{-i\alpha|x|} = e^{-i\mathrm{Re}\alpha|x|}e^{-|\mathrm{Im}\alpha||x|}$, *where the term* $e^{-i\mathrm{Re}\alpha|x|}$ *gives the propagating wave and the second term give the exponential dissipation, growing with the modulus of* $\mathrm{Im}\alpha$.

Proof. Theorem 3 with condition (14) ensures that $J_{min}(\omega) \to 0$ for $\omega \to +\infty$. Let us prove it for a fixed admissible domain Ω. Let us again consider (10) taking a frequency sequence $(\omega_j)_{j \in \mathbb{N}^*}$ such that $\omega_j \to +\infty$ and denoting by u_j the solution of problem (8) with $\omega = \omega_j$. Thanks to the compactness of the trace operator Tr [2], from (14) it follows that for $j \to +\infty$ $\frac{\mathrm{Tr}\, h_j}{\omega_j^2} \to 0$ in $L^2(\Gamma)$. From (14) we also have $\frac{f_j}{\omega_j^2} \to 0$ in $L^2(\Omega)$. In addition, if the sequence $(\|u_j\|_{V(\Omega)})_{j \in \mathbb{N}^*}$ is bounded, then $\frac{1}{\omega_j^2}\|u_j\|_{V(\Omega)} \to 0$. Since for all admissible Ω (which are bounded!) we have the homogeneous Dirichlet condition on Γ_D, then for all Ω it holds the Poincaré inequality, ensuring also the boundness of $(\|u_j\|_{L^2(\Omega)_{j \in \mathbb{N}^*}})$:

$$\|u_j\|^2_{L_2(\Omega)} \leq C_\Omega \|u_j\|^2_{V(\Omega)}.$$

Thus, taking the real part of (10)

$$\|u_j\|^2_{L^2(\Omega)} \quad = \quad \frac{1}{\omega_j^2}\|u_j\|^2_{V(\Omega)} \quad + \quad \frac{1}{\omega_j^2}\int_\Omega \mathrm{Re}(f_j\overline{u}_j)\mathrm{d}x \quad - \quad \frac{1}{\omega_j^2}\int_\Gamma \mathrm{Re}(\mathrm{Tr}\, h_j\overline{\mathrm{Tr}\, u_j})\mathrm{d}m_d,$$

we can passe to the limit on j and obtain that $\|u_j\|^2_{L^2(\Omega)} \to 0$ for $j \to +\infty$.

Hence, let us prove that the sequence $(\|u_j\|_{V(\Omega)})_{j\in\mathbb{N}^*}$ is bounded. By the linearity of the Helmholtz problem, for all $j \in \mathbb{N}$ we set $u_j = u_j^f + u_j^h$, where u_j^f is the solution of the Helmholtz problem with $\mathrm{Tr}\, h_j = 0$ on Γ and u_j^h is the solution of the Helmholtz problem with $f_j = 0$. Taking the imaginary part of (10), we obtain that

$$\lim_{j\to+\infty} \|\,\mathrm{Tr}\, u_j^h\|_{L^2(\Gamma)} \leq \lim_{j\to+\infty}\left(\frac{\|\,\mathrm{Tr}\, h_j\|_{L^2(\Gamma)}}{|\,\mathrm{Im}\,\alpha_j|}\right) = 0,$$

i.e. $\mathrm{Tr}\, u_j^h \to 0$ in $L^2(\Gamma)$. As the trace operator is compact from $V(\Omega)$ to $L^2(\Gamma)$ [2], this implies that $u_j^h \rightharpoonup 0$ in $V(\Omega)$, which finally implies that the sequence $(\|u_j^h\|_{V(\Omega)})_{j\in\mathbb{N}^*}$ is bounded.

Let us show that $\|u_j^f\|_{V(\Omega)} \to 0$ for $j \to +\infty$. Since $h_j = 0$, the variational formulation becomes: for all $\phi \in V(\Omega)$

$$(u_j^f, \phi)_{V(\Omega)} - \omega_j^2(u_j^f, \phi)_{L^2(\Omega)} + i\,\mathrm{Im}\,\alpha_j(\mathrm{Tr}\, u_j^f, \mathrm{Tr}\,\phi)_{L^2(\Gamma)} = -(f_j, \phi)_{L^2(\Omega)}.$$

For all $j \in \mathbb{N}$ we have a sequence of equivalent inner products on $V(\Omega)$:

$$\forall (v, w) \in V(\Omega)\times V(\Omega) \quad (v, w)_{j,V(\Omega)} = (\nabla v, \nabla w)_{L^2(\Omega)} + \mathrm{Re}\,\alpha_j(\mathrm{Tr}\, v, \mathrm{Tr}\, w)_{L^2(\Gamma)},$$

and, since by (14) $\mathrm{Re}\alpha \to c_r \geq 0$, the limit inner product is also equivalent and is denoted by

$$\forall (v, w) \in V(\Omega)\times V(\Omega) \quad (v, w)_{\infty,V(\Omega)} = (\nabla v, \nabla w)_{L^2(\Omega)} + c_r(\mathrm{Tr}\, v, \mathrm{Tr}\, w)_{L^2(\Gamma)}.$$

The case $c_r = 0$ is allowed thanks to the validity on $V(\Omega)$ of the Poincaré inequality. Thus, there exists a sequence $(c_j)_{j\in\mathbb{N}}$ of strictly positive real numbers such that $c_j \to 1$ for $j \to +\infty$ and $c_j\|u\|_{\infty,V(\Omega)} \leq \|u\|_{j,V(\Omega)}$ for all $u \in V(\Omega)$.

Hence, for all $j \in \mathbb{N}$ the Riesz representation Theorem ensures the existence of a linear bounded operator $A_j : L^2(\Omega) \to V(\Omega)$ such that for $v \in L^2(\Omega)$

$$\forall \phi \in V(\Omega) \quad (v, \phi)_{L^2(\Omega)} = (A_j v, \phi)_{j,V(\Omega)}.$$

As in addition, there exists a linear bounded operator $A : L^2(\Omega) \to V(\Omega)$ such that for $v \in L^2(\Omega)$

$$\forall \phi \in V(\Omega) \quad (v, \phi)_{L^2(\Omega)} = (Av, \phi)_{\infty,V(\Omega)},$$

by (14) $A_j \to A$ for $j \to +\infty$, *i.e.* the sequence $(\|A_j\|)_{j\in\mathbb{N}}$ is bounded. Thus, if S is the compact operator of the inclusion of $V(\Omega)$ to $L^2(\Omega)$, then the variational formulation can be rewritten in the following form:

$$\forall \phi \in V(\Omega) \quad \Big((Id - \omega_j^2 A_j \circ S + i\,\mathrm{Im}\,\alpha_j A_j \circ S \circ \mathrm{Tr})u_j^f, \phi\Big)_{j,V(\Omega)} = (-A_j f_j, \phi)_{j,V(\Omega)}.$$

For all j the operator $T_j = A_j \circ S - i\frac{\operatorname{Im}\alpha_j}{\omega_j^2} A_j \circ S \circ \operatorname{Tr} : V(\Omega) \to V(\Omega)$ is obviously compact by the composition of the continuous and compact operators, thus the image of $Id - \omega_j^2 T_j$ is closed in $V(\Omega)$. Knowing that for $(h_j, f_j) = (0,0)$ there exists the unique solution $u_j = 0$ for all j (since $|\operatorname{Im}\alpha_j| > 0$ for all j), we have that $\operatorname{Ker}(Id - \omega_j^2 T_j) = \{0\}$. Since in addition $\operatorname{Im}(Id - \omega_j^2 T_j) = V(\Omega)$, *i.e.* for all $g_j \in V(\Omega)$ there exists a unique solution $u_j^f \in V(\Omega)$ (see also Theorem 3), the linear operator $(Id - \omega_j^2 T_j)^{-1}$ is well defined and is also a linear continuous operator, by the Banach Theorem. Thus, for bounded or unbounded sequence $(\|T_j\|)_{j\in\mathbb{N}}$ depending on the limit properties of $\frac{|\operatorname{Im}\alpha_j|}{\omega_j^2}$ for $j \to +\infty$, we obtain

$$\|u_j^f\|_{\infty, V(\Omega)} \leq \frac{1}{c_j}\|u_j^f\|_{j, V(\Omega)} \leq \frac{\|A_j\|\|f_j\|_{L^2(\Omega)}}{c_j \omega_j^2 \|\frac{1}{\omega_j^2} Id - T_j\|} \to 0 \quad \text{if } j \to +\infty.$$

Consequently, we have proved that $u_j \rightharpoonup 0$ in $V(\Omega)$ for $j \to +\infty$.

In Theorem 4 we impose the decay conditions (14) on the domain D, since it is fixed and contains all admissible Ω. Thus, by the continuity of the trace $V(D) \to V(\Omega)$, conditions (14) ensure the damping of the acoustical energy (see also Example 3.1 in Ref. [23], from where $J(\Omega)(\omega) = \frac{1}{\omega^2}\|u\|^2_{V(\Omega)}$)

$$J(\Omega)(\omega) = \|u\|^2_{L_2(\Omega)} \to 0 \text{ as } \omega \to +\infty.$$

Hence, the same is true for $J_{\min}(\omega)$.

Let us now prove the existence of an ε-optimal domain $\hat{\Omega}_0 \in U_{ad}(\Omega_0)$ on an maximal interval $[\omega_0, \omega_1]$ with $\omega_1 \geq 2\omega_0$ for a sufficiently large ε. It turns on the question how to approximate a continuous function on a compact, here $J_{\min}(\omega)$ on $[\omega_0, 2\omega_0]$, by its value in one point. Thanks to Remark 2, for all $\varepsilon > 0$ there exists $\delta(\varepsilon) > 0$ such that for all ω satisfying $|\omega^* - \omega| < \delta$, a domain Ω^*, optimal for ω^*, is ε-optimal on $]\omega^* - \delta, \omega^* + \delta[$. Thus, taking $\omega^* = \frac{3\omega_0}{2}$, the question is in the possibility to have $\delta \geq \frac{\omega_0}{2}$.

As $J_{\min}(\omega)$ is a continuous function on the compact $[\omega_0, 2\omega_0]$, there exists a frequency $\omega_0^* \in [\omega_0, 2\omega_0]$ giving the value

$$J_{\min}(\omega_0^*) = \frac{1}{2}\left(\max_{[\omega_0, 2\omega_0]} J_{\min}(\omega) + \min_{[\omega_0, 2\omega_0]} J_{\min}(\omega)\right).$$

Therefore, if Ω^* is optimal on ω_0^*, *i.e.* $J(\Omega^*)(\omega_0^*) = J_{\min}(\omega_0^*)$, then for all

$$\varepsilon > \|J_{\min}(\omega) - J_{\min}(\omega_0^*)\|_{C([\omega_0, 2\omega_0])} + \|J(\Omega^*)(\omega) - J(\Omega^*)(\omega_0^*)\|_{C([\omega_0, 2\omega_0])} =: \delta_0 \qquad (15)$$

the triangular inequality shows that the domain Ω^* is ε-optimal on $[\omega_0, 2\omega_0]$ with the maximal interval of ε-optimality $[\omega_0, \omega_1] \supset [\omega_0, 2\omega_0]$.

Obviously, if we minimize the distance $\|J(\Omega^*)(\omega) - J(\Omega^*)(\omega_0^*)\|_{C([\omega_0, 2\omega_0])}$ on the set of optimal domains for ω_0^*, we have

$$\begin{aligned}\inf_{\Omega^*} \|J(\Omega^*)(\omega) - J(\Omega^*)(\omega_0^*)\|_{C([\omega_0, 2\omega_0])} &\geq \|J_{\min}(\omega) - J_{\min}(\omega_0^*)\|_{C([\omega_0, 2\omega_0])} \\ &= \frac{1}{2}\left|\max_{[\omega_0, 2\omega_0]} J_{\min}(\omega) - \min_{[\omega_0, 2\omega_0]} J_{\min}(\omega)\right| := r,\end{aligned}$$

and hence by (15) δ_0 cannot be less than $2r$, which gives a limit of the precision. For instance, for $r_0 < r$ there does not exists $\omega_0^* \in [\omega_0, 2\omega_0]$, such that

$$\|J_{\min}(\omega) - J_{\min}(\omega_0^*)\|_{C([\omega_0,2\omega_0])} \leq r_0.$$

If $J_{\min}(\omega)$ is constant on $[\omega_0, 2\omega_0]$, then the limit precision r becomes equal to zero:

$$\forall \omega \in [\omega_0, 2\omega_0] \quad |J_{\min}(\omega) - \frac{1}{\omega_0}\int_{\omega_0}^{2\omega_0} J_{\min}(\omega)d\omega| = 0.$$

The converse is also true: if for all $\varepsilon > 0$ a fixed domain Ω^* is ε-optimal on a compact interval $[\omega_a, \omega_b]$, then $J_{\min}(\omega)$ is constant on $[\omega_a, \omega_b]$.

By Assumption 2 and Remark 3 $\ell_{\min}(\hat{\Omega}_0) = \frac{\pi}{\omega_0^*} = \frac{\lambda_0^*}{2}$, which is, by its definition, less or equal to $\frac{\lambda_0}{2}$ and larger or equal to $\frac{\lambda_0}{4}$.

Now, on frequency intervals of the form $[2^k\omega_0, 2^{k+1}\omega_0]$ let us consider the corresponding limit precisions

$$r_k := \frac{1}{2}\left|\max_{[2^k\omega_0, 2^{k+1}\omega_0]} J_{\min}(\omega) - \min_{[2^k\omega_0, 2^{k+1}\omega_0]} J_{\min}(\omega)\right|.$$

Since $J_{min}(\omega) \to 0$ for $\omega \to +\infty$, *i.e.* J_{min} converges towards a constant value, thus $r_k \to 0$ for $k \to +\infty$. Hence, it is easier to approximate $J_{\min}$ (with more precision) for high than for low frequencies. Consequently, there exist a finite number $K \in \mathbb{N}$ of the frequency ranges of the form $[2^k\omega_0, 2^{k+1}\omega_0]$ and $k_0 \in \mathbb{N}$, such that if $r_{k_0} = \max_{i=1,\dots,K} r_i$ is the minimal precision on these K intervals, then for all $k \geq k_0$ the limit precisions in higher frequencies are better: $r_k \leq r_{k_0}$.

Therefore, taking ε_0 large enough, such that $\varepsilon_0 \geq 2r_{k_0} \geq 0$ and $\varepsilon_0 > \delta_0$, to prove the theorem it is sufficient to show that for all $\varepsilon > \varepsilon_0$ there exists a sequence $(\Omega_n)_{n=1,\dots N-1} \subset U_{ad}(\hat{\Omega}_0)$, such that

1. for all $\omega \in [\omega_0, 2^n\omega_0]$ ($n \leq N-1$), the domain Ω_n is ε-optimal with characteristic scales $\ell_k(\Omega_n) \leq \frac{\lambda_0}{2^{k+1}}$ for $k = 1, \dots, n$, where $\ell_n(\Omega_n) = \ell_{min}(\Omega_n)$;

2. there exists Ω^*, which is equal to $\Omega_N \in U_{ad}(\hat{\Omega}_0)$ if $N < +\infty$ and which is a fractal (an (ε, ∞)-domain) if $N = +\infty$ with $\ell_k(\Omega^*) \leq \frac{\lambda_0}{2^{k+1}}$ for $k \in \mathbb{N}^*$, such that $\Omega_n \overset{*}{\rightharpoonup} \Omega^*$ in the class of locally uniform domains (see Definition 2), which means:

$$\forall \omega \in [\omega_0, \omega_{\max}[\quad \forall \eta > 0 \quad \exists M(\omega, \eta) > 0 : \ \forall n \geq M(\omega, \eta) \\ |J(\Omega_n)(\omega) - J(\Omega^*)(\omega)| < \eta,$$

and finally conclude that this Ω^* is ε-optimal on $[\omega_0, \omega_{\max}[$ (by point 1):

$$\forall \omega \in [\omega_0, \omega_{\max}[\quad |J(\Omega^*)(\omega) - J_{min}(\omega)| < \varepsilon.$$

Let us fix $\varepsilon > \varepsilon_0$. For instance, a sequence of n-times wavelength preserving optimal domains $\hat{\Omega}_n$ based on $\hat{\Omega}_0$ for the frequency ω_0 verifies the properties 1–2. Indeed, we have constructed a domain $\hat{\Omega}_0 \in U_{ad}(\Omega_0)$ with $\ell_{min}(\hat{\Omega}_0) = \frac{\lambda_0^*}{2} \in [\frac{\lambda_0}{4}, \frac{\lambda_0}{2}]$, such that it is

ε-optimal on a maximal interval $[\omega_0, \omega_0^e[\supset [\omega_0, 2\omega_0]$. Let now, $\hat{\Omega}_1 \in U_{ad}(\Omega_0)$ be optimal on $\omega_1^* \in [2\omega_0, 4\omega_0]$, such that

$$J_{\min}(\omega_1^*) = \frac{1}{2}\left(\max_{[2\omega_0,4\omega_0]} J_{\min}(\omega) + \min_{[2\omega_0,4\omega_0]} J_{\min}(\omega)\right) \quad \text{and} \quad d_H(\hat{\Omega}_1, \hat{\Omega}_0) \leq \frac{\lambda_1^*}{4}.$$

Thus, $\hat{\Omega}_1$ is a 1-time wavelength preserving optimal domain based on $\hat{\Omega}_0$ for the frequency ω_0 (see Definition 8). Consequently, by point 3 of Proposition 2, the domain $\hat{\Omega}_1$ is ε-optimal on $[\omega_0, 2\omega_0]$ and by the optimality on the frequency ω_1^* and by the fact that $\varepsilon \geq 2r_1$, $\hat{\Omega}_1$ is also ε-optimal on $[2\omega_0, 4\omega_0]$. Hence, $\hat{\Omega}_1$ is ε-optimal on $[\omega_0, 4\omega_0]$. Taking each time optimal domains on the frequencies ω_k^* with the restriction $d_H(\hat{\Omega}_k, \hat{\Omega}_{k-1}) \leq \frac{\lambda_k^*}{4}$, we obtain a sequence of n-times wavelength preserving optimal domains $(\hat{\Omega}_n)_{n=1,\ldots,N-1}$ based on $\hat{\Omega}_0$ for the frequency ω_0. Proposition 2 ensures point 1 and that $\Omega^* = \Omega_{N-1}$ if N is finite.

For $N = +\infty$ we have for all $n \in \mathbb{N}$ $d_H(\hat{\Omega}_n, \hat{\Omega}_{n+1}) \leq \frac{1}{4}\frac{\lambda_0}{2^{n+1}}$, and thus, independently of $n \in \mathbb{N}$, by Proposition 2, $d_H(\hat{\Omega}_0, \hat{\Omega}_n) \leq \frac{\lambda_0}{4}$. For all $n \geq 1$ the domain $\hat{\Omega}_n \in U_{ad}(\hat{\Omega}_0)$ is ε-optimal on $[\omega_0, 2^n\omega_0]$ with $\hat{d}(\hat{\Omega}_n, \hat{\Omega}_{n+1}) \to 0$ for $n \to +\infty$. Hence point 2 holds by construction and also by the compactness results of Ref. [25] (Theorem 5.1 p. 205 and Theorem 2.4 ii) p.59). $\square$

Remark 6 *To be coherent with numerical results of Section 4, Theorem 4 is given in the two-dimensional case. But, thanks to the general properties of the wave propagation, the physical principle in Assumption 1 obviously holds for the three dimensional case too, which directly implies Theorem 4 also for three-dimensional domains: to be the most efficient to dissipate the acoustical energy in $\mathbb{R}^2$ or $\mathbb{R}^3$ for almost all frequencies, the boundary Γ must be fractal.*

4 Numerical experiments

For all numerical tests, presented below, are performed in the same conditions as described in Section 6 of Part I [23].

4.1 Illustrations for Assumption 1 and Theorem 4

Time dependent energy decay We consider the three cavities $\Omega = \Omega_0 \sqcup \Omega_1 =]0, 1[\times]-2, 2[$, partially shown on Fig. 3 with two homogeneous media, air (lower part) and a porous material (upper part), separated by an internal boundary Γ_i, $i = 0, 1, 2$. To preserve the volume of each medium and to model the increasing irregularity of the interface, as compared to the plane Γ_0 (at $y = 0$), we choose Γ_1 and Γ_2 as the first two fractal generations of a symmetric element. The external boundary $\partial\Omega$ is supposed to be perfectly rigid (Neumann boundary condition). Air is considered as a lossless medium, and the porous medium (ISOREL) is considered as a dissipative homogeneous medium. As it was mentioned in [23], using the ideas of Hamet [13], we can describe the wave propagation in the porous material by a damped wave equation involving the physical characteristics of the material: the porosity ϕ, the tortuosity α_h and the resistivity to

the passage of air σ. Denoting by c_0 and ρ_0 the sound velocity and the density in the air, and by $\gamma_p = 7/5$ the ratio of specific heats, the equations of wave propagation in Ω are given by

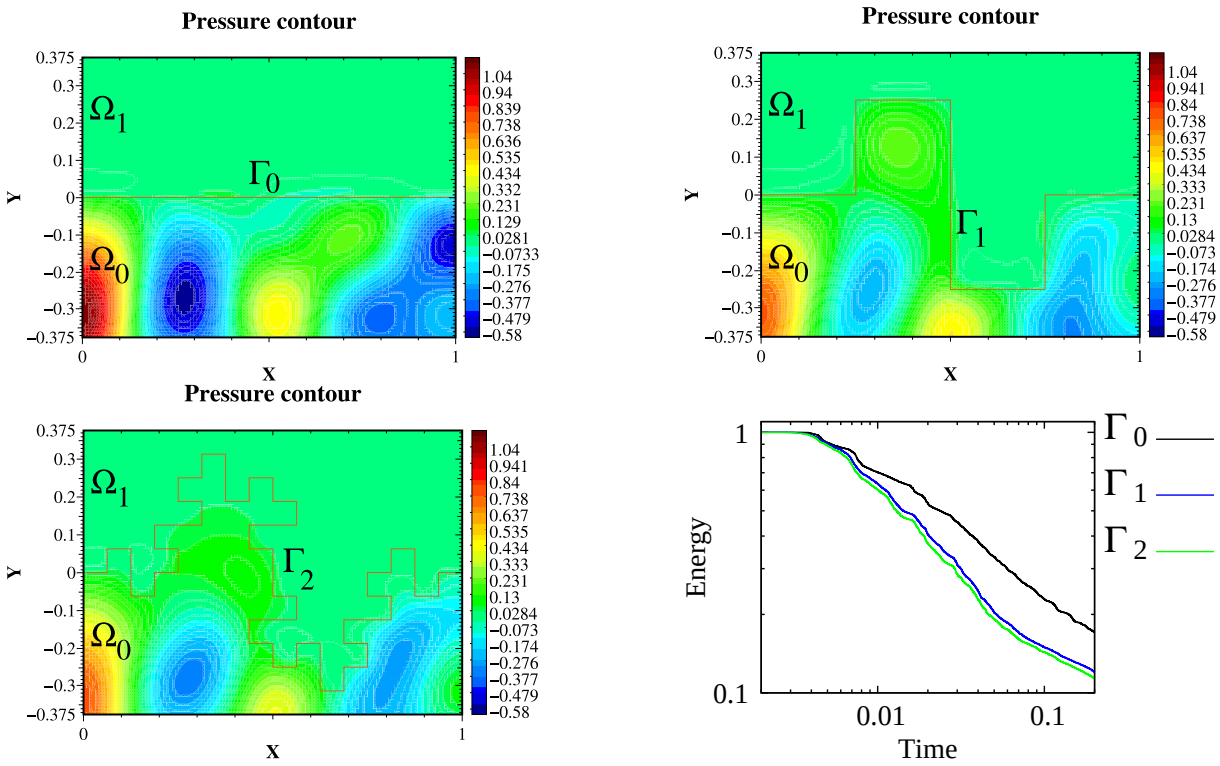

Figure 3: Pressure contours at $t = 0.01$ in cavities with an internal boundary of different Minkowski fractal generations (from left to right and top to bottom: Γ_0 (flat), Γ_1 and Γ_2) and the corresponding energy damping. The size of the mesh is 128×512.

$$\xi(x)\partial_t^2 u + a(x)\partial_t u - \nabla \cdot (\mu(x)\nabla u) = 0 \quad \text{in } \Omega = \Omega_0 \sqcup \Omega_1, \tag{16}$$

with $\xi(x) = \frac{1}{c_0^2}$, $a(x) = 0$, $\mu(x) = 1$ in the air and $\xi(x) = \frac{\phi\gamma_p}{c_0^2}$, $a(x) = \sigma\frac{\phi^2\gamma_p}{c_0^2\rho_0\alpha_h}$, $\mu(x) = \frac{\phi}{\alpha_h}$ in the porous medium. Equation (16) is supplemented with the following no-jump conditions through Γ_i

$$[u]_{\Gamma_i} = [\mu\nabla u \cdot n]_{\Gamma_i} = 0$$

and with an initial data chosen as a Gaussian, centered in a fixed point $x_0 = (0.75, -1.5)$ of Ω_0:

$$u|_{t=0} = \frac{1}{\delta\sqrt{2\pi}} e^{-\frac{|x-x_0|^2}{2\delta^2}}, \quad \partial_t u|_{t=0} = 0,$$

where $\delta = 0.1$. Such a choice of δ ensures that $\text{supp}(u|_{t=0})$ is extremely small outside Ω_0. Equation (16) is the wave equation in the air ($a = 0$), and is the damped wave

equation [3, 9] ($a \neq 0$) in the porous medium. This provides the energy decay (see [23] section 2):

$$\frac{1}{2}\frac{d}{dt}\left(\int_\Omega \big[\xi(\partial_t u)^2 + (\mu\nabla u)\cdot\nabla u\big]dx\right) = -\int_\Omega a(\partial_t u)^2 dx. \tag{17}$$

We discretize Eq. (16) in a way which mimics the energy dissipation (17), and which is an adaptation to damped acoustic waves of the finite volume method presented in Ref. [15]. Let u_i^n be the discretized pressure in the control volume i at time $n\Delta t$, then we write

$$\xi\frac{u_i^{n+1}-2u_i^n+u_i^{n-1}}{\Delta t^2} + a\frac{u_i^{n+1}-u_i^{n-1}}{2\Delta t} - [\nabla\cdot(\mu\nabla u^n)]_i = 0,$$

so that the energy like functional $E^{n+1/2} := \frac{1}{2}\Big(\int_\Omega \xi\big(\frac{u^{n+1}-u^n}{\Delta t}\big)^2 \mathrm{d}x + \int_\Omega \mu\nabla u^n\cdot\nabla u^{n+1}\mathrm{d}x\Big)$ is damped as

$$\frac{1}{\Delta t}\left(E^{n+1/2}-E^{n-1/2}\right) = -\int_{\Omega_1} a\Big(\frac{u^{n+1}-u^{n-1}}{2\Delta t}\Big)^2 \mathrm{d}x.$$

Fig. 3 shows that an irregular shape of the internal boundary can significantly increase the dissipation properties of the porous medium ($\Gamma_{1,2}$ as compared to Γ_0). The energy damping by Γ_1, compared to the damping performances of Γ_0, is much better and we notice that the wavelength λ of the wave, created by the initial data, is comparable (twice bigger) to the characteristic length scale size of the geometry Γ_1. At the same time, the small difference in the energy decays corresponding to the internal boundaries Γ_1 and Γ_2 confirms the hypothesis of Assumption 1: the wave does not penetrate in the smallest geometry parts of size $\lambda/8$, but the wave still keeps a good penetration for the scales of the order $\lambda/2$ as for Γ_1. This finally implies that the shape of the internal boundary does not need to be "too complicated" for being an efficient acoustic absorbent for a fixed frequency.

Frequency optimization results For all numerical tests, presented below, we consider the rectangle $\overline{D} = [0,3]\times[0,1]$, and suppose that D always contains the domain Ω, on which we solve the Helmholtz equation. The boundaries Γ_N and Γ_D are fixed, and Γ is the moving boundary inside of $\overline{G} = [\frac{3}{2},3]\times[0,1]$. The initial $\Omega_0 =]0,2[\times]0,1[$ has a flat boundary Γ_0 fixed at $x = 2$.

First we calculate the values of J

$$J(\Omega)(\omega) = \int_\Omega |u|^2\mathrm{d}x + \int_\Omega |\nabla u|^2\mathrm{d}x + \mathrm{Re}(\alpha)\int_\Gamma |u|^2\mathrm{d}s$$

for a range of frequencies for the flat shape Ω_0, for instance for $\omega\in[2400,4000]$. Let us fix a frequency $\omega_0 = 3170$, corresponding to a local maximum of J. For this fixed ω_0 we have $\alpha = 23.7699 - 24.8367i$ (see SM of Part I [23]).

Then we perform two numerical tests, taking different initial domains Ω_0 in the shape optimization algorithm: the flat geometry of Γ (see Fig. 4) and a non-flat Γ (see Fig. 5) with the smallest characteristic geometric size $\ell_{\min}(\Omega_0)$ much smaller than the wavelength $\lambda = \frac{\ell}{2}$. The optimal shape on Fig. 4 has a mean value of shape scale length of order $\frac{\ell}{4}$, *i.e.* $\ell(\Omega_{16}) = \frac{\lambda}{2}$. The optimal shape $\hat{\Omega}_{10} = \Omega^*_{\mathrm{opt}}$ on Fig. 5 keeps the largest characteristic

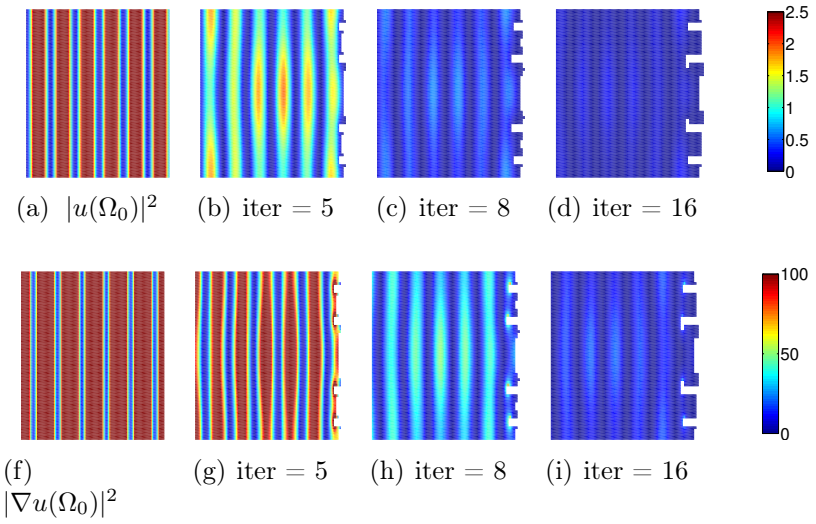

(a) $|u(\Omega_0)|^2$ (b) iter $= 5$ (c) iter $= 8$ (d) iter $= 16$

(f) $|\nabla u(\Omega_0)|^2$ (g) iter $= 5$ (h) iter $= 8$ (i) iter $= 16$

Figure 4: From the top to the bottom the values of $|u|^2$ and $|\nabla u|^2$ on the domains (from the left to right) Ω_0 (with the flat Γ), Ω_5, Ω_8 and Ω_{16} respectively with the same scale of colors in each row. The domain Ω_0 is the initial shape and the domain Ω_{16} is the optimal shape for $\omega = 3170$.

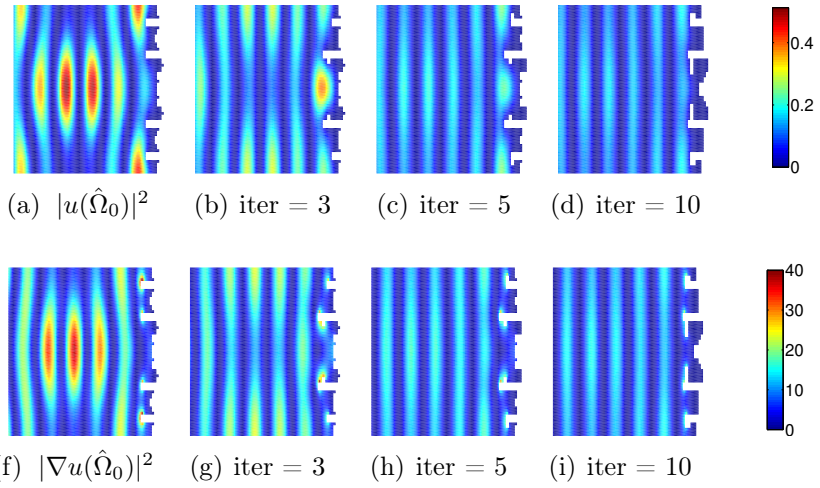

(a) $|u(\hat{\Omega}_0)|^2$ (b) iter $= 3$ (c) iter $= 5$ (d) iter $= 10$

(f) $|\nabla u(\hat{\Omega}_0)|^2$ (g) iter $= 3$ (h) iter $= 5$ (i) iter $= 10$

Figure 5: From the top to the bottom the values of $|u|^2$ and $|\nabla u|^2$ on the domains (from the left to right) $\hat{\Omega}_0$, $\hat{\Omega}_3$, $\hat{\Omega}_5$ and $\hat{\Omega}_{10}$ respectively with the same scale of colors in each row. The domain $\hat{\Omega}_0$ is the initial shape and the domain $\hat{\Omega}_{10}$ is the optimal shape for $\omega = 3170$.

geometrical size of order $\frac{\lambda}{2}$ ($\ell(\Omega^*_{\rm opt}) = \frac{\lambda}{2}$) and for smaller scales $\Omega^*_{\rm opt}$ is in a small neighborhood of $\Omega^{\rm flat}_{\rm opt}$.

Fig. 6 illustrates Point 1 of Proposition 1: $\Omega^*_{\rm opt}$ differs from $\Omega^{\rm flat}_{\rm opt}$ only through small scale details and both are optimal at ω_0. In addition, Fig. 6 shows the existence of a frequency interval $[\omega_1, \omega_2]$, including $\omega_0 = 3170$, for which the optimal shapes $\Omega^{\rm flat}_{\rm opt}$ and

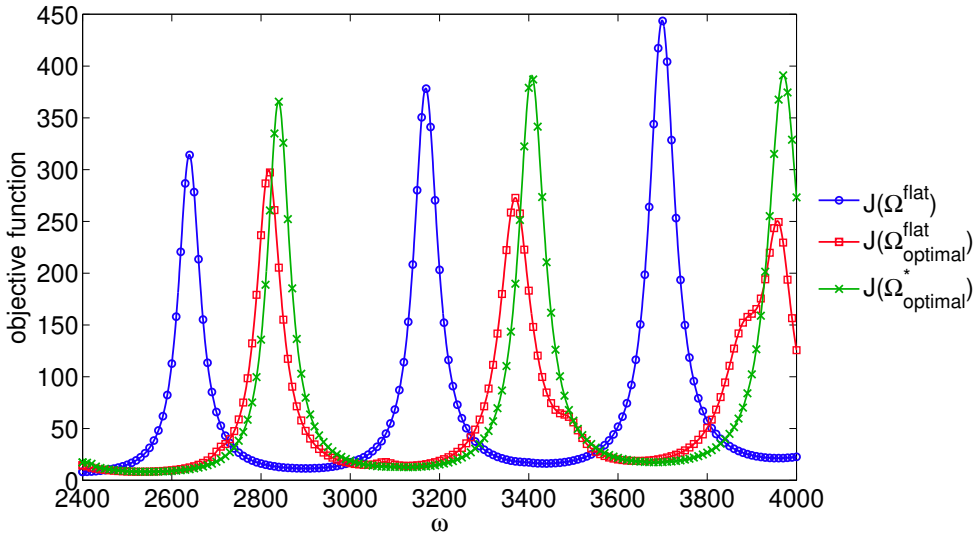

Figure 6: The objective function J as a function of ω for the flat shape $\Omega_0 = \Omega^{\text{flat}}$ given by the line with circles, for the optimal shape $\Omega_{16} = \Omega^{\text{flat}}_{\text{opt}}$ (see Fig. 4) given by the line with squares, and for the optimal shape $\hat{\Omega}_{10} = \Omega^*_{\text{opt}}$ (see Fig. 5) given by the line with stars. The optimal domains $\Omega^{\text{flat}}_{\text{opt}}$ and Ω^*_{opt} are $J(\Omega_0)(\omega_0)/J(\Omega^*_{\text{opt}})(\omega_0) = 27.5$ times better for the energy dissipation than the flat shape Ω_0.

Ω^*_{opt} are ε-optimal by the continuity of the functional J_1 on ω_0.

4.2 Optimized "simple" wall for a large range of frequencies

In this subsection, we are searching an ε-optimal shape of the wall Ω, minimizing the acoustical energy $J(\Omega)(\omega) = \int_\Omega |u|^2 \mathrm{d}x$ in a large range of frequencies with the simplest possible design. Let us fix the range of frequencies for the energy dissipation: $\omega \in [3000, 6000]$.

As in Section 4.1, we fix the frequency $\omega_0 = 3170$ of a local maximum of J on $\Omega_{\text{flat}} =]0,2[\times]0,1[$. We perform the shape optimization algorithm for this frequency, taking as the initial shape Ω_0, given on Fig. 7, and we obtain Ω_1, optimal at $\omega = 3170$. Noticing that all local maxima of $J(\Omega_1)$ are smaller than the local maxima of $J(\Omega_{\text{flat}})$ (see Fig. 8), we choose Ω_1 as the initial domain and restart the optimization algorithm, minimizing in the neighborhood of Ω_1 the sum of functionals $\sum_{k=1}^{3} J(\Omega)(\omega_k)$, where $\omega_1 = 3410$, $\omega_2 = 4025$ and $\omega_3 = 4555$ are the local maxima of $J(\Omega_1)$. This minimization gives the optimal shape Ω_2, such that

1. Ω_2 is ε-optimal in the neighborhood of ω_k for $k = 0, 1, 2, 3$;
2. all local maxima of $J(\Omega_2)$ are smaller than the local maxima of $J(\Omega_1)$.

Choosing $\omega_4 = 3625$ and $\omega_5 = 4240$, corresponding to the local maxima of $J(\Omega_2)$, we take Ω_2 as the initial domain and restart the optimization algorithm, minimizing $J(\Omega)(\omega_4) + J(\Omega)(\omega_5)$ to obtain the optimal shape Ω_3, such that

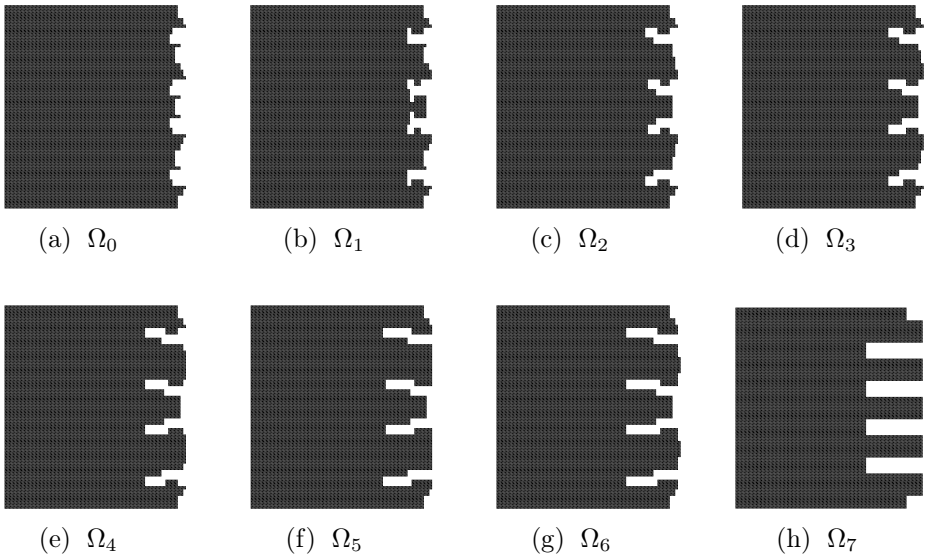

(a) Ω_0 (b) Ω_1 (c) Ω_2 (d) Ω_3

(e) Ω_4 (f) Ω_5 (g) Ω_6 (h) Ω_7

Figure 7: Shapes, which are used in the optimization algorithm process: from left to right in the top line- Ω_0 (the initial shape), Ω_k, $k = 1, 2, 3$, and from left to right in the bottom line - Ω_k, $k = 4, 5, 6, 7$. The domain Ω_7 is generated manually in the aim to simplify Ω_6 (the final ε-optimal shape).

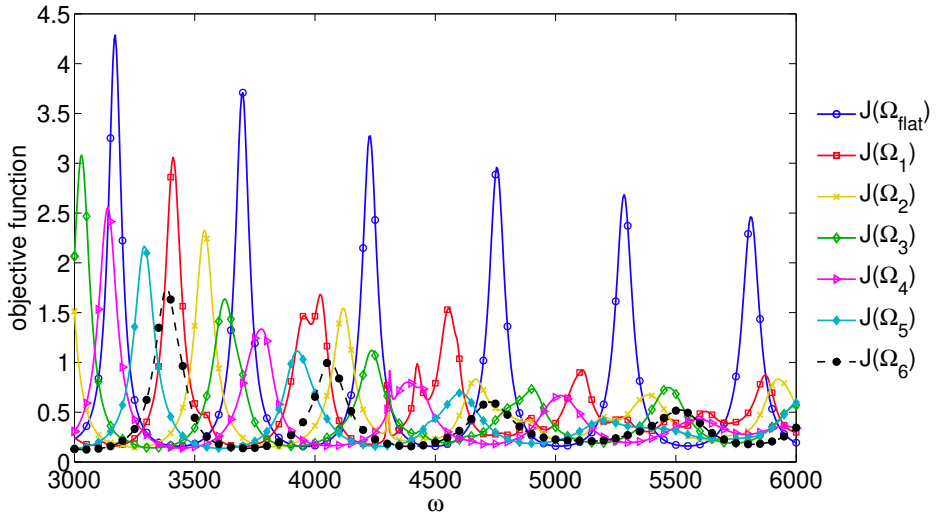

Figure 8: The values of the objective function $J(\Omega_0)$ ($A = 1, B = 0, C = 0$) for the flat shape as a function of $\omega \in [3000, 6000]$ are presented by the line with circles, the values of $J(\Omega_1)$ (see Fig. 7 for the shape of Ω_1) are presented by the line with squares, of the values $J(\Omega_2)$ by the line with stars, those of $J(\Omega_3)$ by the line with empty rhombus, those of $J(\Omega_4)$ by the line with arrows, those of $J(\Omega_5)$ by the line with full rhombus, and those of $J(\Omega_6)$ by the black dashed line.

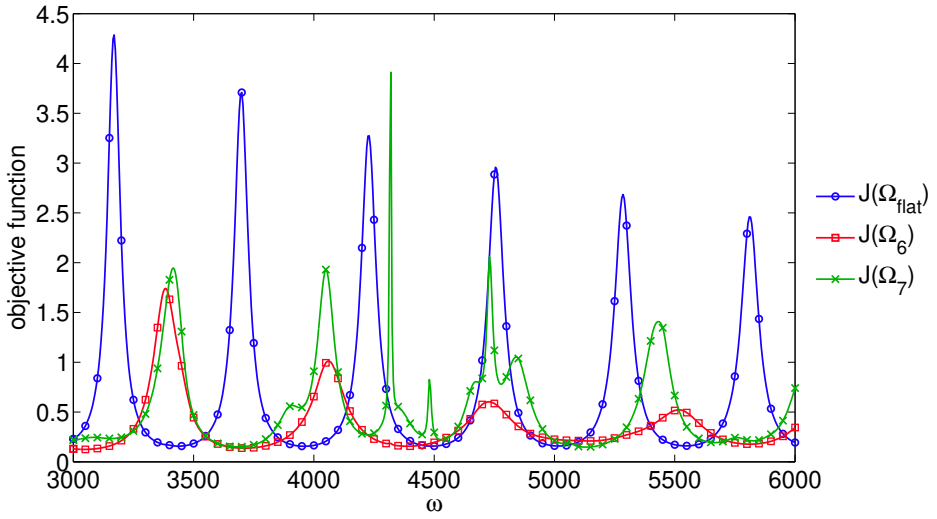

Figure 9: Comparison of the dissipative properties of the flat shape Ω_{flat}, the optimal Ω_6 and of its simplification Ω_7. The values of $J(\Omega_{\text{flat}})$, of $J(\Omega_6)$ and of $J(\Omega_7)$ ($A = 1, B = 0, C = 0$) as functions of $\omega \in [3000, 6000]$ are given by the lines with circles, squares and stars respectively. Examples of the energy distribution for three values of frequencies illustrating the three typical cases: $J(\Omega_6) \approx J(\Omega_7)$, $J(\Omega_6) < J(\Omega_7)$ and $J(\Omega_7)$ has its local maximum, are given in Appendix A.

1. Ω_3 is ε-optimal in the neighborhood of ω_k for $k = 0, \ldots, 5$;

2. all local maxima of $J(\Omega_3)$ are smaller than the local maxima of $J(\Omega_2)$.

We iterate this process up to Ω_6 and we are stopped by the restriction that Γ must be contained by the area $\overline{G} = [\frac{3}{2}, 3] \times [0, 1]$.

The shape of Ω_6 contains multiscale details, which ensures the dissipative performances of the wall in a large range of frequencies (see Fig. 8). Thinking about the demolding process of wall construction, we simplify the geometry of Ω_6, deleting the multi-scales and keeping only the largest characteristic scale of Ω_6 (see the domain Ω_7 (generated by hand) on Fig. 7). As we can see from Fig. 9, since we have kept almost unchanged the largest characteristic geometric size $\ell(\Omega_6) \approx \ell(\Omega_7)$, the energy dissipation is almost the same in the corresponding range of frequencies (see red and green lines for $[3000, 3700]$ on Fig. 9). As all smaller scale details have been deleted, the shape of Ω_7 is not so good as the shape of Ω_6 to dissipate higher frequencies (see lines with squares and stars for $[3700, 6000]$ on Fig. 9). Hence, Fig. 9 shows that the compromises between two desired properties "to be the most dissipative" (as Ω_6 here) and "to be simple to construct" (on the example of Ω_7) is not too bad, especially if we know the most important frequencies to dissipate.

5 Conclusion

The well-posedness for the Helmholtz equation with a damping on the boundary was obtain in the class of n-sets, which generalizes the case of Lipschitz boundary to d-sets, including fractals for $n-1<d<n$. In the framework of a noise barrier optimization, we have introduced the concept of the ε-optimal domains and have shown that for an efficient dissipation of the energy in a large band of frequencies, the ε-optimal domain must have a multiscale boundary geometry. More precisely, we have proved that an ε-optimal domain for all frequencies exists and, to be the most dissipative, it has a fractal boundary with a characteristic scale for a fractal generation $\lambda/2$. We have illustrated the theoretical results by numerical examples. With the purpose to find the most efficient and the simplest ε-optimal domain, easy to construct, we show numerically that if we simplify the obtained ε-optimal shape, by deleting the smaller scales of the geometry, the new shape is efficient in the frequencies corresponding to its characteristic geometry scale length, but no more efficient in the higher frequencies.

A Complement to Section 4.2

Figs. 10–12 show the energy distribution for three values of frequencies illustrating the three typical cases: $J(\Omega_6)\approx J(\Omega_7)$, $J(\Omega_6)<J(\Omega_7)$ and $J(\Omega_7)$ has its local maximum (see Fig. 9).

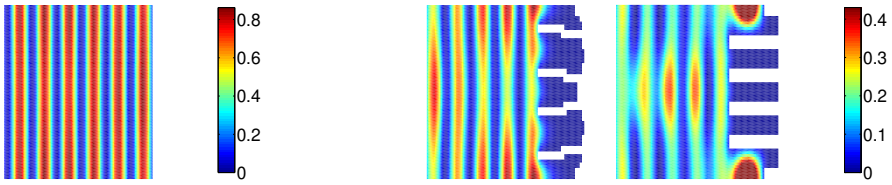

(a) $|u(\Omega_{\text{flat}})|^2$ (c) $|u(\Omega_6)|^2$ (d) $|u(\Omega_7)|^2$

Figure 10: Energy distribution in Ω_{flat}, Ω_6 and Ω_7 respectively for $\omega=3235$, corresponding to the case, when $J(\Omega_6)\approx J(\Omega_7)$ are almost the same (precisely $J(\Omega_6)=0.2841$, $J(\Omega_7)=0.2829$)

References

[1] G. Allaire, *Conception optimale de structures*, 58 Mathématiques et Applications, Springer, 2007.

[2] K. Arfi and A. Rozanova Pierrat, *Dirichlet-to-Neumann or Poincaré-Steklov operator on fractals described by d-sets*, DCDS-S Special issue on "Variational convergence and Degeneracies in PDEs: fractal domains, composite media, dynamical boundary conditions", to appear, (2017).

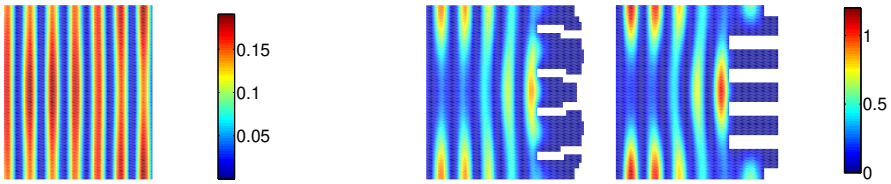

(a) $|u(\Omega_{\text{flat}})|^2$ (c) $|u(\Omega_6)|^2$ (d) $|u(\Omega_7)|^2$

Figure 11: Energy distribution in Ω_{flat}, Ω_6 and Ω_7 respectively for $\omega = 3495$, corresponding to the case, when $J(\Omega_6) = 0.4767$ and $J(\Omega_7) = 0.5077$ take slight different values.

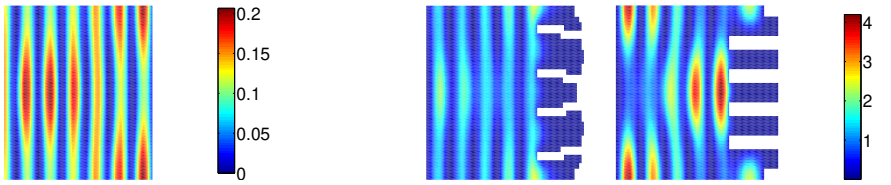

(a) $|u(\Omega_{\text{flat}})|^2$ (c) $|u(\Omega_6)|^2$ (d) $|u(\Omega_7)|^2$

Figure 12: Energy distribution in Ω_{flat}, Ω_6 and Ω_7 respectively for $\omega = 3415$, the frequency, which yields a local maximum of the objective function on the domain Ω_7.

[3] M. Asch and G. Lebeau, *The Spectrum of the Damped Wave Operator for a Bounded Domain in $\mathbb{R}^2$*, Experimental Mathematics, 12 (2003), pp. 227–241, https://doi.org/10.1080/10586458.2003.10504494.

[4] C. Bardos, D. Grebenkov, and A. Rozanova Pierrat, *Short-time heat diffusion in compact domains with discontinuous transmission boundary conditions*, Math. Models Methods Appl. Sci., 26 (2016), pp. 59–110, https://doi.org/10.1142/{S}0218202516500032.

[5] C. Bardos and J. Rauch, *Variational algorithms for the Helmholtz equation using time evolution and artificial boundaries*, Asymptotic Analysis, 9 (1994), pp. 101–117.

[6] M. Bodin, *Characterisations of function spaces on fractals*, PhD thesis, 2005.

[7] R. Capitanelli, *Mixed Dirichlet-Robin problems in irregular domains*, Comm. to SIMAI Congress, 2 (2007), https://doi.org/10.1685/{C}{S}{C}06035.

[8] R. Capitanelli, *Asymptotics for mixed Dirichlet–Robin problems in irregular domains*, Journal of Mathematical Analysis and Applications, 362 (2010), pp. 450–459, https://doi.org/10.1016/j.jmaa.2009.09.042.

[9] S. Cox and E. Zuazua, *The rate at which energy decays in a damped string*, Communications in Partial Differential Equations, 19 (1994), pp. 213–243, https://doi.org/10.1080/03605309408821015.

[10] J. Dardé, *Méthodes de quasi-réversibilité et de lignes de niveau appliquées aux problèmes inverses elliptiques*, PhD thesis, 2010.

[11] M. J. Gander, L. Halpern, and F. Magoulès, *An optimized Schwarz method with two-sided Robin transmission conditions for the Helmholtz equation*, International Journal for Numerical Methods in Fluids, 55 (2007), pp. 163–175, https://doi.org/10.1002/fld.1433.

[12] P. Hajłasz, P. Koskela, and H. Tuominen, *Sobolev embeddings, extensions and measure density condition*, Journal of Functional Analysis, 254 (2008), pp. 1217–1234, https://doi.org/10.1016/j.jfa.2007.11.020.

[13] J.-F. Hamet and M. Berengier, *Acoustical characteristics of porous pavements: a new phenomenological model*, Internoise 93,Louvain, Belgique, (1993), pp. 641–646.

[14] A. Henrot and M. Pierre, *Variation et optimization de formes. Une analyse géométrique*, Springer, 2005.

[15] F. Hermeline, S. Layouni, and P. Omnes, *A finite volume method for the approximation of Maxwell's equations in two space dimensions on arbitrary meshes*, Journal of Computational Physics, 227 (2008), pp. 9365–9388, https://doi.org/10.1016/j.jcp.2008.05.013.

[16] D. A. Herron and P. Koskela, *Uniform, Sobolev extension and quasiconformal circle domains*, J. Anal. Math., 57 (1991), pp. 172–202, https://doi.org/10.1007/{B}{F}03041069.

[17] P. W. Jones, *Quasi onformal mappings and extendability of functions in Sobolev spaces*, Acta Mathematica, 147 (1981), pp. 71–88, https://doi.org/10.1007/{B}{F}02392869.

[18] A. Jonsson and H. Wallin, *Function spaces on subsets of* $\mathbb{R}^n$, Math. Reports 2, Part 1, Harwood Acad. Publ. London, 1984.

[19] A. Jonsson and H. Wallin, *The dual of Besov spaces on fractals*, Studia Mathematica, 112 (1995), pp. 285–300.

[20] A. Jonsson and H. Wallin, *Boundary value problems and brownian motion on fractals*, Chaos, Solitons & Fractals, 8 (1997), pp. 191–205, https://doi.org/10.1016/{S}0960-0779(96)00048-3.

[21] M. R. Lancia, *A Transmission Problem with a Fractal Interface*, Zeitschrift für Analysis und ihre Anwendungen, 21 (2002), pp. 113–133, https://doi.org/10.4171/{Z}{A}{A}/1067.

[22] J. Lions and E. Magenes, *Non-Homogeneous Boundary Value Problems and Applications*, vol. 1, Berlin: Springer-Verlag, 1972.

[23] F. Magoulès, T. P. K. Nguyen, P. Omnès, and A. Rozanova Pierrat, *Optimal absorption of acoustical waves by a boundary, part 1*, Submitted, (2017).

[24] J. Marschall, *The trace of Sobolev-Slobodeckij spaces on Lipschitz domains*, Manuscripta Math, 58 (1987), pp. 47–65, https://doi.org/10.1007/{B}{F}01169082.

[25] F. Murat and J. Simon, *Optimal Design*, Optimization Techniques Modeling and Optimization in the Service of Man Part 2, Lecture Notes in Computer Science, 41 (2005), pp. 52–62.

[26] H. Wallin, *The trace to the boundary of Sobolev spaces on a snowflake*, Manuscripta Math, 73 (1991), pp. 117–125, https://doi.org/10.1007/{B}{F}02567633.